Talanta 219 (2020) 121269

Contents lists available at ScienceDirect

Talanta

journal homepage: www.elsevier.com/locate/talanta

Sensors in heart-on-a-chip: A review on recent progress

Kyoung Won Cho[a,b,1], Wang Hee Lee[a,c,1], Byung-Soo Kim[c], Dae-Hyeong Kim[a,b,c,*]

[a] Center for Nanoparticle Research, Institute for Basic Science (IBS), Seoul, 08826, Republic of Korea
[b] Interdisciplinary Program for Bioengineering, Seoul National University, Seoul, 08826, Republic of Korea
[c] School of Chemical and Biological Engineering, Institute of Chemical Processes, Seoul National University, Seoul, 08826, Republic of Korea

ARTICLE INFO

Keywords:
Heart-on-a-chip
Flexible electronics
Biosensors
Drug screening
Electrophysiology

ABSTRACT

Drug-induced cardiotoxicity is a major problem in drug discovery. Many approaches to efficient drug screening have been developed, including animal testing *in vivo* and cell testing *in vitro*. However, due to intrinsic difference between species, animal-based toxicity testing cannot comprehensively determine the potential side effects in subsequent human clinical trials. Furthermore, conventional *in vitro* assays are costly and labour-intensive, and require numerous tests. Therefore, it would be necessary to develop heart-on-a-chips made with advanced materials and soft bioelectronic fabrication techniques that offer fast, efficient, and accurate sensing of cardiac cells' behaviors *in vitro*. In this review, we introduce two key sensing methods in heart-on-a-chip for physical and electrical measurements. First, optical (*e.g.*, direct and calcium imaging, and fluorescent, laser-based, and colorimetric sensing) and electrical (*e.g.*, impedance, strain, and crack sensing) sensors that record the contractility of cardiomyocytes are reviewed. Subsequently, various sensors composed of rigid planar/three-dimensional electrodes, soft/flexible electronics, and nanomaterial-based transistors to monitor extracellular and intracellular electrophysiological potentials are discussed. A brief overview of future technology and comments on the current challenges conclude the review.

1. Introduction

The heart is one of the most vital and least regenerative organs [1]. Cardiac diseases [2] are popular subjects of study for scientists, particularly in the field of pharmacology [3], as a major obstacle to drug discovery is drug-induced cardiotoxicity [4,5]. New drugs must undergo a variety of tests, such as *in vitro* cell tests [6,7] and *in vivo* animal/clinical studies [8–13] to confirm a lack of harmful side effects [14], as well as to evaluate the therapeutic efficacy [15]. While drug candidates go through numerous tests, the failure rate can be up to 60% due to the lack of efficient and effective screening platforms [16–18]. In the past, newly developed drugs have been screened using animal models [5] before proceeding to the subsequent stage (*i.e.*, the human trial) [19]. This stage of animal testing incurs a high proportion of the total costs and labour [20,21]. However, many of these approaches have failed in the transition from animal testing to human trials [22] because animal models can present misleading results due to species difference [23,24] and can fail to predict harmful effects in heart tissues (*i.e.*, cardiotoxicity) that can occur in human trials [25].

There is a need to develop a reliable platform to culture and monitor cardiac cells so that the detailed biological aspects of heart diseases can be scrutinized *in vitro* [26–28]. *In vitro* assays have been utilized in drug screening [29] to remedy the limitations of animal testing. However, conventional assays are time-consuming and labour-intensive to screen numerous samples. The cells for the assays can be harvested directly from animals or derived from human embryonic stem cells, which may involve ethical issues. In addition, there is a lack of appropriate tools for monitoring cells *in vitro* in real time. To address the limitations of conventional *in vitro* assays, an engineered heart-on-a-chip [30,31] integrated with monitoring capabilities has been proposed. Recent technological advances in flexible and soft electronics have propelled the development of the high performance *in vitro* platform [32] for sensing cardiac cells' properties. This integrated platform converges cell biology [33], nanomaterials [34–37], and fabrication technologies [38,39] to precisely record the mechanical and electrical cues [40,41] of the cardiac cells *in vitro* and mimic the spatiotemporal microenvironment of the heart [42–44].

In this review, we introduce the recent advances in the bioelectronic technologies [45–47], focusing in particular on the heart-on-a-chip [48]. The review is largely categorized into two sensing methods that include the sensing of contractility [49] and the extracellular and intracellular action potentials of cardiomyocytes. This review begins by

* Corresponding author. Center for Nanoparticle Research, Institute for Basic Science (IBS), Seoul, 08826, Republic of Korea.
E-mail addresses: calvin@snu.ac.kr (K.W. Cho), wwhh0315@snu.ac.kr (W.H. Lee), byungskim@snu.ac.kr (B.-S. Kim), dkim98@snu.ac.kr (D.-H. Kim).
[1] K. W. Cho and W. H. Lee contributed equally to this work.

https://doi.org/10.1016/j.talanta.2020.121269
Received 27 March 2020; Received in revised form 14 May 2020; Accepted 2 June 2020
Available online 16 June 2020
0039-9140/

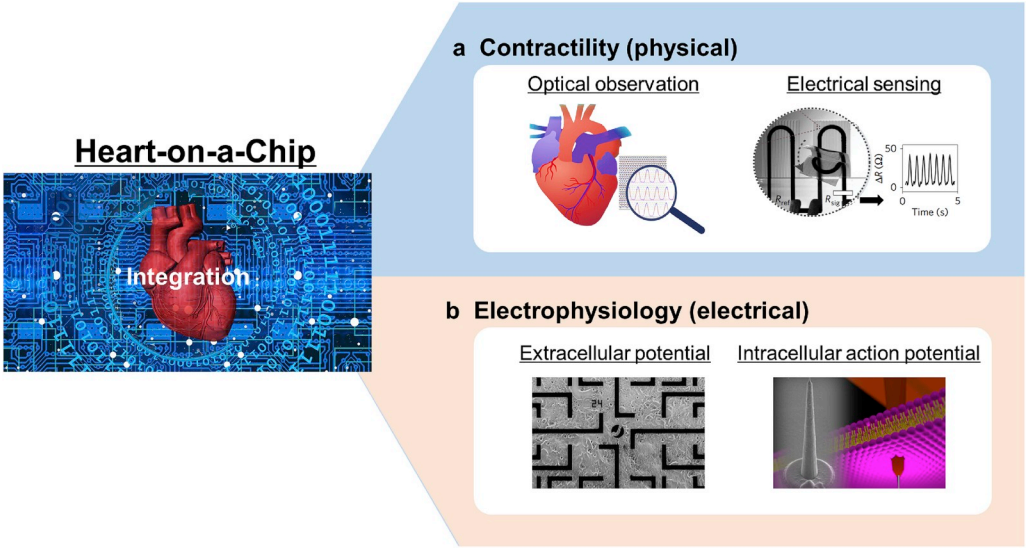

Fig. 1. Overview of heart-on-a-chip converging electronics and cardiac cells. Two modes of sensing in heart-on-a-chip include a) contractility (physical) and b) electrophysiology (electrical) of cardiomyocytes. Reproduced with permission [56,57,82,156,157]. Copyright 2014 American Association for the Advancement of Science, Copyright 2019 Elsevier, Copyright 2017 Nature Publishing Group, Copyright 2020 John Wiley & Sons, Copyright 2016 John Wiley & Sons.

highlighting the optical sensing method of contractility [50], which is one of the most widespread and basic techniques for recording the contraction of beating cells. Subsequently, flexible electrical signal-based sensors, such as an impedance sensor [51] and a strain gauge for monitoring contractility, are discussed (Fig. 1a). Next, we discuss various electrodes that monitor the extracellular electrophysiological signals of cardiomyocytes with a particular emphasis on the integration technology of advanced soft and flexible electronic devices to improve the sensitivity and sensing reliability in cellular environments *in vitro*. Finally, methodologies for recording intracellular cardiac action potentials integrated with advanced nanomaterials and device fabrication techniques for enhanced signal strength with minimal cell membrane damages are introduced (Fig. 1b). The integration of advanced soft bioelectronics with cardiac cell biology is expected to dramatically improve the heart-on-a-chip technology to provide a cost-effective and efficient screening platform of drug-induced cardiotoxicity tests.

2. Cardiac contractility assay

Cardiac contractility can be monitored to discern healthy and diseased cardiomyocytes [52]. It indicates the various functions of cardiomyocytes by monitoring cardiac systolic functions, such as the frequency [53], force [54], and synchronization [55] of cardiac contractions. Precise analysis of cardiac contractility would aid to understand the fundamental mechanisms of heart function [56], which would facilitate studies on the therapeutic efficacy and unexpected cardiotoxicity of new drug candidates [57]. In this section, we discuss on the recent progress in the cardiac contractility sensor development, focusing on sensors based on optical and electrical measurements.

2.1. Optical observation of the cardiac contractility

One of the most widely studied methods to record the cardiac contractility is the direct observation of cardiomyocytes' contraction and relaxation *via* optical apparatus [58]. Optical sensing is regarded a high-speed, accurate, and versatile method of detecting cardiac contractility due to the high sensitivity of light-based signals and its independence from other types of sensing methods [50], such as electrophysical and/or electrochemical sensors [59]. Representative optical sensing methods for cardiac contractility include video analysis [60], traction force microscopy (TFM) [61], calcium imaging [62], laser sensing [63], atomic force microscopy (AFM) [64], and colorimetric sensing [65].

The most primitive method for measuring cardiac contractility is the direct optical imaging to measure discrete sarcomere lengths *via* microscopy [66]. The variations in length of individual sarcomeres exhibit cardiac contractility; however, direct optical imaging inevitably involves imprecise measurement due to experimental errors [58]. Video analyses using micropost arrays have been developed to obtain precise contractility measurements and monitoring of the three-dimensional contractile force [60]. A flexible micropost array made of polydimethylsiloxane (PDMS) is easily fabricated using soft lithography of the double-casting procedures with the stiffness enough to endure the contractile force of cardiomyocytes (Fig. 2a left). The array of the microposts with the height of 2 μm and spacing of 6 μm acts as the reference point to obtain cardiac contractility by measuring their displacement. The contraction of cardiomyocytes that adhere to the tips of the microposts causes deflection of the microposts, which is then recorded by video (Fig. 2a right). The actual distance of the displacement for each micropost is measured *via* the video analysis (Fig. 2b). The measurement of the cardiac contraction with an aid of the micropost array and video recording can increase the accuracy compared to direct observation and measurement of the sarcomere length. Furthermore, each post of the micropost array can also measure the contractile forces. The peak force is identified by calculating the maximum force during each contraction, while the twitch force is calculated by the difference between the peak force and the passive tension of each contraction.

Although the video analysis using micropost array provides precise means to quantify cardiac contractility, it cannot be utilized as drug screening platform due to its time-consuming nature, its inability to measure in real time, and its possibility to deform cardiomyocytes' morphology [67] far from the natural *in vivo* environment. Recently, TFM is actively researched and considered as a non-invasive, *in situ*, and simple method [61] for cardiac contractility monitoring [68]. Unlike micropost array or a cantilever, TFM allows the recording of the cardiomyocytes with native-like cellular behavior such as enhanced adhesion and alignments. TFM utilizes fluorescent beads as fiducial markers which are immobilized within the elastic substrate such as hydrogel or PDMS. Cells are then cultured on the protein-functionalized surface of a thin elastic substrate (Fig. 2c). The contractions can be measured by tracking the position of the fluorescent beads, which indicate the elastic displacement of the hydrogel (Fig. 2d).

Since the bead is immobilized within the culture substrate, the topographical and mechanical property of the substrate can be easily modified to bio-mimic the native environment *in vivo*. Specifically, cardiomyocytes are organized and aligned *in vivo*, yet are randomly patterned when cultured *in vitro*. Providing a controlled cell-substrate interaction in the nanoscale level (*i.e.*, substrate patterning) is

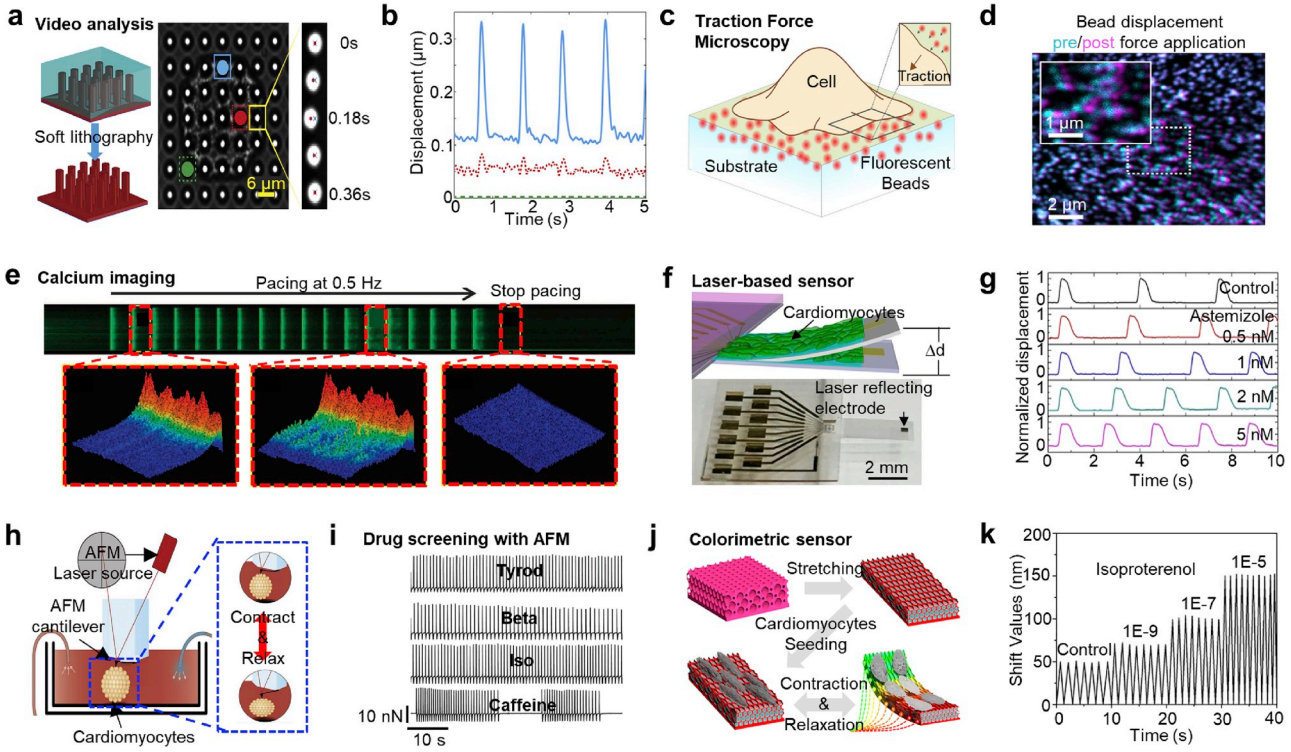

Fig. 2. Optical observation of cardiac contractility. a) Video analysis for cardiac contractility monitoring using PDMS microposts fabricated with soft-lithography (left) and actual video image of contractility analysis, which is the top view of the microposts (right) b) Plot showing the displacement of a single cardiac contraction obtained by video analysis. Posts near the edge of cardiomyocytes (blue) deform much dynamically than posts near the middle of cardiomyocytes (red). Posts which are not attached to cardiomyocytes (green) rarely deform. Reprinted with permission [60]. Copyright 2016 Elsevier. c) Schematic illustration of the traction force microscopy. Traction forces generated by the cardiac cells can be calculated *via* imaging the displacement of the fluorescent beads within the substrate. d) Confocal fluorescent image showing displaced bead positions before (cyan) and after (magenta) the cardiac contraction. Reprinted with permission [61]. Copyright 2018 Elsevier. e) Calcium ion signaling in cardiac cells before, during, and after pacing (top) and magnified images of calcium ion sparks before, during, and after pacing (bottom). Reprinted with permission [62]. Copyright 2014 American Association for the Advancement of Science. f) Schematic illustration (top) and photographic image (bottom) of the laser-based measurement based on the displacement of a cantilever including laser-reflecting electrodes. g) Plot of displacement of the cantilever measured by the laser measurement of cardiac contraction under different concentrations of astemizole treatment. Reprinted with permission [63]. Copyright 2019 American Chemical Society. h) Schematic illustration of atomic force microscopic measurement of contractility. i) Plot of cardiac contractility treated with beta-adrenergic receptor antagonist metoprolol (Beta), the beta-adrenergic agonist isoproterenol (Iso), and the calcium discharger caffeine triggering arrhythmia, compared to the baseline signal standardized in the Tyrod buffer. Reprinted with permission [64]. Copyright 2016 Elsevier. j) Schematic illustration of a colorimetric sensor integrated on a cantilever. k) Plot showing the displacement and frequency of colorimetric sensors treated with different concentrations of isoproterenol. Reprinted with permission [65]. Copyright 2019 American Chemical Society. (For interpretation of the references to color in this figure legend, the reader is referred to the Web version of this article.)

important to acquire contraction as well as action potentials from cardiomyocytes *in vitro* as similar to those *in vivo* as possible [69]. TFM analysis enables detection of the force change during diastole and systole of cardiomyocytes, and the force distribution in any part of cardiomyocytes can be calculated at any time. Although TFM exhibits high utility for cardiac contractility monitoring, the method does present certain limitations, such as the lack of a consistent resolution of the obtained contractile forces due to the random distribution of fluorescent beads. In addition, TFM is unable to record the time points during monitoring and cannot detect vertical contractile forces [67].

Calcium imaging utilizes fluorescent dyes [70] to measure calcium ion concentrations in the cytoplasm of cardiomyocytes as an indicator for contractility [71]. This method offers high-throughput analyses for drug screening [72]. Jian et al. have monitored cardiac contractility through calcium imaging. Ca^{2+} signaling in cardiomyocytes is measured before, during, and after pacing (Fig. 2e). Initially, cardiomyocytes exhibit very few Ca^{2+} sparks before pacing at 0.5 Hz. The number of Ca^{2+} sparks increases during paced contraction. When the pacing stops, the Ca^{2+} sparks clear out immediately. Although calcium imaging achieves high-throughput analysis of cardiac contractility, it is still an indirect contractility measurement.

A cantilever is an efficient monitoring platform for the precise recording of cardiac contraction in tissue level. For direct and real-time contractility measurements, cantilevers with laser sensors have been introduced [73]. The laser-reflecting electrode on the cantilever surface gauges the displacement of the cantilever induced by the cardiac contraction (Fig. 2f). This system can monitor change in the cardiac contractility depending on the concentration of astemizole, a medicine for hypertension and heart rhythm disorders, showing potential as a facile drug screening platform of cardiac cells (Fig. 2g). Such a laser-based sensor enables facile cardiac contractility measurements, but has a distinct limitation in that heat generation by the laser irradiation can harm the metabolism of the cardiomyocytes [67].

When combined with AFM, cantilevers can serve as biomechanical sensors for cardiac contractility, allowing for accurate measurements and monitoring of other mechanical properties in addition to contractility simultaneously [67]. Fig. 2h shows the setup of AFM cantilever devices for cardiac contractility monitoring (left) and the contractile movements of cardiomyocyte clusters measured by the AFM cantilever (right). The interaction force between the beating cardiomyocytes and the AFM tip can be recorded in real time. Treatment with a beta-adrenergic receptor antagonist metoprolol, a beta-adrenergic agonist isoproterenol, and a calcium discharger caffeine changes the contractile force of the cardiomyocytes, compared to the baseline signal

standardized in a Tyrod buffer (Fig. 2i). The AFM cantilever device has distinct limitations in that a laser must be incorporated into the measurement procedures, and invasive contact must be made on the cardiomyocytes [74].

Recently, a colorimetric sensor for cardiac contractility monitoring has been developed [65]. This sensor enables facile and efficient detection without exposure to high-energy light and/or direct mechanical contacts on cells [75]. Shang et al. have developed a biohybrid colorimetric sensor based on anisotropic inverse opal substrate elliptical macropores filled with a hydrogel. The color of the biohybrid sensor changes as the seeded cardiomyocytes contract (Fig. 2j). For the demonstration of a drug screening platform, different concentrations of isoproterenol are injected to the microfluidic system and an increase in the wavelength shift is observed (Fig. 2k). Due to the utilization of high-energy light such as laser is not required, the cardiomyocytes cultured on a calorimetric sensor can be monitored without any physical damage (*i.e.*, heat) and maintains high viability even after the monitoring.

2.2. Electrical detection of cardiac contractility

Electrical signal-based contractility sensors (*e.g.*, impedance, strain [76], and crack-based sensors) enable facile, real-time, and long-term recording of cardiac contractility [77]. Electrical impedance sensing has been utilized to monitor growth, spreading, and differentiation of cells [7]. Recently, impedance sensors have been used to monitor cardiomyocyte contractility by recording changes in the impedance (Fig. 3a top). As cells grow and cover the electrode of the impedance sensor, the current flow through electrodes of the sensor generally lowers [78]. Then, as the cardiomyocytes contract, the gap between the electrode and the cell layer changes and the impedance fluctuates (Fig. 3a bottom, 3b).

Although impedance sensing enables real-time and long-time monitoring, it has the potential to induce undesired side effects due to the direct exposure of the applied current flow to the cells [67]. In recent years, strain sensors have been spotlighted for cardiac contractility sensors owing to their flexibility [79] that arise from their thin film structure. The strain caused by cardiomyocyte contraction can be converted into electrical signals, such as change in resistance [80]. Wang et al. have used carbon nanotubes (CNTs) as the strain sensor material and fabricated a CNT sensor-embedded microdevice for drug screening platforms (Fig. 3c). The validation of the strain sensor platform is tested with five drugs: isoproterenol, verapamil, omecamtiv mecarbil, ivabradine, and E4031. Fig. 3d representatively presents the effect of verapamil. The strain sensing exhibits a higher magnitude of the resistance measurements than the impedance sensing.

Embedding strain sensors into cantilevers can mimic the three-dimensional native structure [81] of the myocardium. Lind et al. have fabricated a cantilever structure, strain sensor, groove, and culture well simultaneously *via* multi-material three-dimensional printing [82]. The cantilever deflects as cardiomyocytes seeded on the cantilever surface contract, and the strain sensor measures the contractility of the cardiomyocytes simultaneously (Fig. 3e). The carbon black strain sensor embedded in the cantilever measures the contractility of cardiomyocytes in real time (Fig. 3f left), and the strain gauge shows a maximum at systole and minimum at diastole of the cardiomyocyte contraction (Fig. 3f right). The integrated culture scaffold that considers the functional, structural and biological aspects of the cardiomyocytes dramatically simplifies the data collection and facilitates efficient long-term cardiac studies [5].

Although 3D printing [83] enables the facile fabrication of strain sensors for cardiac contractility measurements, the strain sensors do possess certain limitations in that they exhibit low sensitivity owing to their low gauge factor [84]. Crack sensors have received considerable attention due to their flexibility [85,86], durability [87], and outstanding mechano-sensitivity. Fig. 3g shows the mechanism of crack sensing for cardiac contractility, which is the driving force of ultrahigh sensitivity and long-term stability of the crack sensor under a culture medium condition. The crack sensor gauge shows a maximum at systole and minimum at diastole of the cardiac tissue contraction and relaxation (Fig. 3h). Compared to piezo-resistive sensors, crack sensors have a signal-to-noise ratio that is 600 times higher, enabling accurate analysis of cardiac contractility. Unlike conventional sensors that lack long-term stability under a culture medium environment, crack sensors maintain the stability of sensing even after 26 days in culture medium.

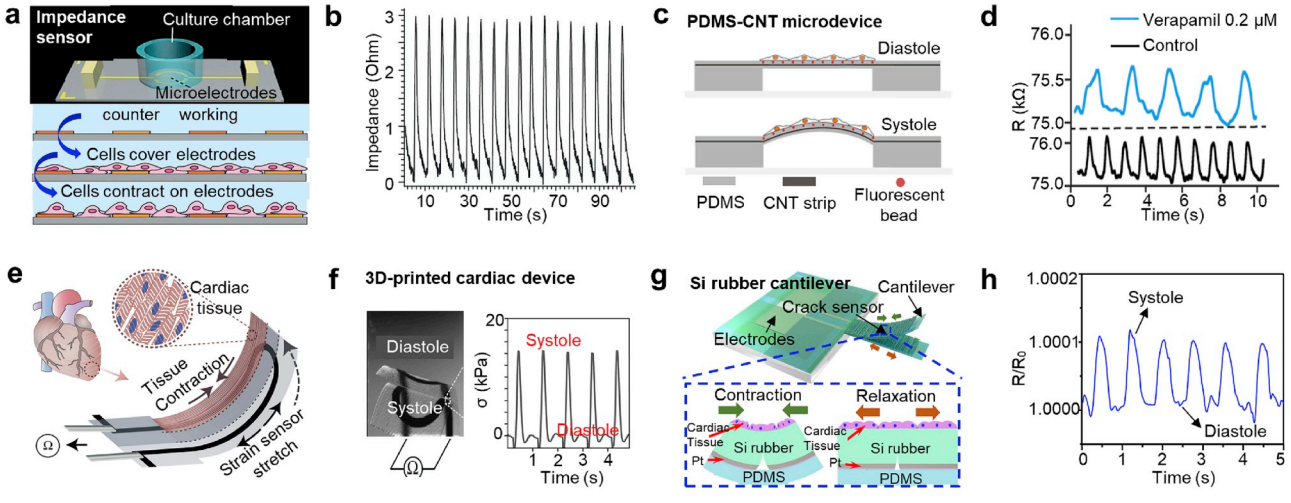

Fig. 3. Electrical detection of cardiac contractility. a) Schematic illustration of impedance-based sensor to record cardiac contraction (top) and contraction of cardiac cells on electrodes (bottom). b) Plot of changes in impedance during cardiac contraction. Reprinted with permission [78]. Copyright 2017 The Royal Society of Chemistry. c) Exploded view of the strain gauge integrated into thin film bridge for contractility assay. d) Plot of resistance changes in cardiac contraction induced by treatment of verapamil. Reprinted with permission [67]. Copyright 2018 American Chemical Society. e) Schematic illustration of a 3D printed cantilever integrated with strain gauge. f) Microscope image of the 3D printed cantilever bending by cardiac contraction (left) and relative resistance changes and corresponding calculated twitch stress recorded from the strain sensor (right). Reprinted with permission [82]. Copyright 2017 Nature Publishing Group. g) Schematic illustration of the crack-induced strain gauge sensor on the cantilever (top) and the details of crack sensor during contraction and relaxation of cardiac cells (bottom). h) Changes in the resistance ratio of the crack sensor during contraction and relaxation of cardiac cells. Reprinted with permission [84]. Copyright 2020 Nature Publishing Group.

3. Sensors for monitoring cardiac action potentials of cardiomyocytes

3.1. Electrodes for extracellular electrophysiology of cardiomyocytes

Cardiomyocytes perform both electrochemical and mechanical activities simultaneously. The precise characterization of the cardiac action potential, in addition to cardiac contractile monitoring, is highly important in the screening of cardiotoxicity [88]. The heart tissue is composed of electrogenic cells called cardiomyocytes, in which the extracellular potential changes as a result of the ionic flow through the cellular membrane [89]. The transmembrane potential of −90 mV at rest is transiently depolarized by the influx of cations, such as sodium and calcium [88]. This change in potential subsequently propagates along the adjacent cell surface. Sensing the cardiac action potential allows for a better understanding of heart tissue behavior and can distinguish normal and malfunctioning heart tissue *in vitro* [90]. Such electrical investigation of cardiac cellular activities can be accomplished using bioelectronics when the surface of the electrode is in close contact with or is inserted into the cell membrane [91]. In this section, various types of bioelectronic sensors that are capable of monitoring the cardiac action potentials of cardiomyocytes are reviewed.

3.1.1. Rigid planar and 3D electrodes

The conventional tool for monitoring the electrophysiology of the heart tissue is the planar microelectrode array (MEA) [92]. The device is typically made of metal electrodes, such as gold and platinum, on a rigid substrate [93]. The array of electrodes allows for multiple sites of the cell culture to be recorded at the same time and the electrical propagation generated in the cultured cardiomyocytes to be mapped [94]. The key to improve the sensitivity of MEA is decreasing the intrinsic impedance of materials [77] and increasing the area of the cell-device interface [95–97]. Carbon-based nanomaterials [98,99] and 2D materials [100] such as graphene have gained attention as novel materials for the fabrication of MEAs due to their excellent electrical property, biocompatibility, and transparency. In particular, the transparency of graphene [101] compared with other metal-based materials offers a strong advantage, as it enables the observation of cells directly at the recording site.

Recently, a graphene-based MEA with an array of 64 electrodes has been developed to record the extracellular action potential of cardiomyocyte-like cells, HL-1 [102] (Fig. 4a top). The detection site is made of CVD-grown graphene and is patterned to a diameter of 10 μm with Au electrodes on a wafer substrate and passivated with polyimide (Fig. 4a bottom). HL-1 cells are cultured on top of the device (Fig. 4b left). Due to the transparent property of graphene, *in situ* observation of the cells *via* optical apparatus such as the phase contrast microscope is possible without sacrificing the cells from either immunostaining or Pt coating for scanning electron microscopy. As the cells contract, the corresponding action potentials in multiple sites of the electrode are simultaneously recorded with high signal-to-noise ratios of 45 ± 22. Also, the delay of signal amplitudes between each channel indicates the signal propagation along the cell culture (Fig. 4b right).

The planar electrode array is considered a stable and non-invasive method for recording the electrophysiology of cardiomyocytes [103,104]. The high-quality and accurate recording of electrophysiological signals in cardiomyocytes is critical and depends heavily on the signal-to-noise ratios of the recording electrodes. Recently, 3D electrodes [105], such as vertical micropillars, have been actively investigated. These 3D electrodes show a higher signal-to-noise ratio compared to conventional planar electrodes because the 3D electrodes have a higher surface area, which decreases the electrode impedance. Cools et al. have reported on a 3D micro-structured electrode made with an aggregated form (well shape) of vertically aligned CNTs [106]. The well-shaped CNTs can be controlled by the condensation and evaporation of the acetone vapor exposed onto the surface of the CNTs, the capillary force of which pulled the CNTs closely together (Fig. 4c top). Furthermore, the van der Waals force between the closely packed CNTs subsequently densifies them into a well-shaped arrangement in which the size of electrode diameter can be controlled (Fig. 4c bottom). Similar to graphene, CNT has a strong advantage as a carbon-based nanomaterial as it exhibits dramatically low electrode impedance and high biocompatibility due to the enhanced electron transfer. This well-shaped formation of the 3D CNT electrode allows to entrap the cell and to significantly increase the surface area of electrode-cell interface unlike a flat electrode which only contacts the cell at the bottom side (Fig. 4d). Due to the 3D structure and shape of well, higher amplitudes in the extracellular recording of the primary cardiomyocytes are observed compared with bare flat electrodes.

3.1.2. Flexible electrodes

The development of an *in vitro* platform to maximally mimic the heart is critical for the reliability of drug-induced cardiotoxicity testing [69,92]. For instance, the alignment of the cardiomyocytes *in vitro* can lead to a higher velocity of the action potential propagation than that of cardiomyocytes cultured with a random orientation. In order to bio-mimic the cardiac environment *in vivo* during electrophysiological recording, the biomimetic cues should be integrated onto the recording electrodes through, for example, the nano-topographical patterning [107]. In addition to the topographical cue of the substrate, the geometrical and mechanical properties of the substrate are also critical to bio-mimic the native heart environment. Cardiomyocytes *in vivo* are organized into a 3D shape and are closely connected each other [108]. In many cases, cells used for *in vitro* testing are cultured as a monolayer. Cells are cultured on a rigid substrate where the modulus of the culture substrate is significantly different from the natural environment *in vivo*. 2D monolayer cell culture can lead to different cellular behaviors compared with 3D cell culture [109]. The culture environment may engender unexpected and different physiological behaviors such as low sarcomere and myofibril formation [110]. To overcome the limitations of monolayer cell culture, cells can be cultured in 3D engineered scaffolds [111] made of various types of materials, such as nanofibers and hydrogels [112,113], that mimic the 3D *in vivo* environment. Moreover, 3D organoid [114] cell culture is an emerging trend in tissue engineering and drug discovery. On the other hand, conventional rigid planar electrodes are incompatible to be integrated within soft engineered scaffold. Therefore, flexible electronics [79,115,116] that improve the quality of the cell-electronics interface by evading the mechanical mismatch to the modulus of the soft substrates are being actively developed [117–119].

Feiner et al. have recently developed an engineered cardiac patch integrated with flexible electronics and a 3D nanocomposite scaffold [120]. The flexibility of this device is advantageous as it can be rolled or folded along with the 3D scaffold while recording the extracellular electrical signals of cardiomyocytes (Fig. 4e). The flexible MEA of 32 electrodes is made of an Au layer encapsulated with SU-8 polymer on a porous network of a SU-8 mesh substrate. In addition, a rough nanoscale layer of titanium nitride is deposited onto the sensing part of the electrode to increase the surface area and cell adhesion. Additionally, the cardiac patch is capable of performing the controlled release of drugs that are incorporated in the polypyrrole film. The thick 3D tissue-scaffold construct (Fig. 4f) is made of the SU-8 mesh that acts as the backbone of the patch (Fig. 4f inset) covered with the electrospun nanocomposite fiber scaffold of polycaprolactone-gelatin. The mechanical property of the flexible electrode is well matched with the soft property of the cells. Therefore, the integration of flexible electronics into an engineered 3D scaffold allows to record the cultured cardiomyocytes without damaging the cells even under deformations.

Although there is a 3D MEA that can wrap around the surface of a single cell to record its signal, Kalmykov et al. have developed a 3D self-rolled biosensor array that can simultaneously perform 3D multisite recording of multicellular spheroids [121] (Fig. 4g, inset for the

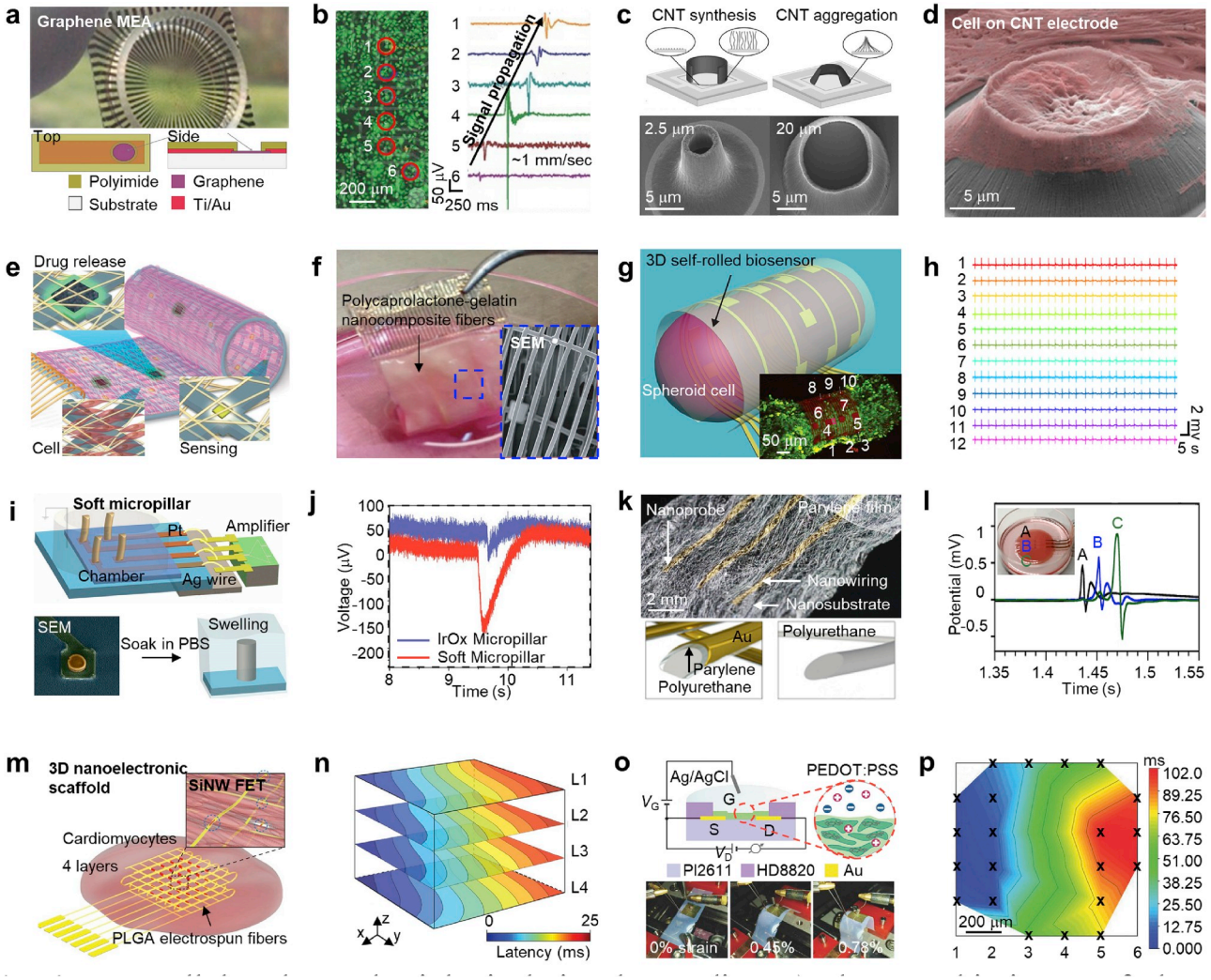

Fig. 4. Extracellular electrophysiological signal recording. a) Photographic image of planar rigid graphene-based MEA (top) and schematic illustration of device configuration (bottom). b) Fluorescent image of HL-1 cells with the locations of recording site (left) and plot of extracellular potential recording of the cell showing the electrical signal propagation (right). Reprinted with permission [102]. Copyright 2017 John Wiley & Sons. c) Schematic illustration showing the process of aggregated formation of 3D CNT electrodes (top) and SEM images of vertically aligned CNTs aggregated as a shape of wells whose diameters are 2.5 μm and 20 μm (bottom). d) Colored SEM image of neonatal rat cardiomyocytes on a single electrode of 3D CNT MEA. Reprinted with permission [106]. Copyright 2016 John Wiley & Sons. e) Schematic illustration of a flexible cardiac patch encompassing capabilities of drug delivery, cell culture, and sensing. f) Photographic image of a cardiac patch with engineered cardiac scaffold. The inset shows SEM image of the cardiac patch without the scaffold. Reprinted with permission [120]. Copyright 2016 Nature Publishing Group. g) Schematic illustration of a 3D self-rolled MEA encapsulating a spheroid of cardiac cells. The inset shows a fluorescent image of the human cardiomyocyte spheroid wrapped with the self-rolled MEA. The number indicates the location of recording sites while two additional sites located at the backside are not shown. h) Plot of electrical signals recorded from multiple sites at all sides of the spheroid. Reprinted with permission [121]. Copyright 2019 American Association for the Advancement of Science. i) Schematic illustration of a soft conductive hydrogel micropillar array (top) and the swelling process of the hydrogel micropillar after soaking in phosphate-buffered saline (PBS) (bottom). j) Plot of signal recorded from the soft hydrogel micropillar electrode and rigid iridium oxide micropillar electrode. Reprinted with permission [126]. Copyright 2018 National Academy of Sciences. k) Microscopic image of an ultrasoft nanomesh electrode (top) and schematic illustrations showing an electrospun polyurethane nanofibers coated with a gold layer (bottom). l) Plot of electrophysiological signals recorded at the sites of A, B, and C, and the photographic image of the nanomesh closely adhered onto the fibrin gel of cardiac cells (inset). Reprinted with permission [127]. Copyright 2019 Nature Publishing Group. m) Schematic illustration of a multilayer silicon nanowired FET array in engineered scaffold composed of electrospun PLGA fibers. n) 3D mapping data of the electrical propagation induced by the cultured cardiomyocytes. Reprinted with permission [131]. Copyright 2016 Nature Publishing Group. o) Schematic illustration of a flexible organic electrochemical transistor (top) and photographic image of the device applied under strains of 0, 0.45, and 0.78% (bottom). p) Heat map of the recorded cardiac electrical signals. The marker of x indicates the recording sites. Reprinted with permission [136]. Copyright 2018 John Wiley & Sons. (For interpretation of the references to color in this figure legend, the reader is referred to the Web version of this article.)

fluorescence microscopic image). The 3D self-rolled MEA is fabricated on a planar layer of a germanium sacrificial layer with a base support of SU-8 polymer. The electrode is deposited and patterned with the chromium, palladium, and gold layers, and the sacrificial layer underneath disintegrates to form a 3D rolling structure. The shape transformation of the rolling is driven by the mismatch of residual strains between different constituent layers in which the tensile stress is generated from palladium and chromium layers. Unlike other flexible electrodes intended to monitor either 2D or 3D cell culture, the self-rolling property of this MEA is suitable for monitoring the multicellular spheroid culture. The human cardiomyocytes are formed into multicellular spheroid during differentiation from the embryonic stem cell. The rod-shaped cell aggregate of embryonic stem cell-derived cardiomyocytes is encapsulated within the self-rolled MEA, which records the electrical activity of the 3D spheroid at 12 recording sites from all sides of the 3D spheroid (Fig. 4h). This enables the electrical propagation of

cardiomyocytes to be measured more accurately, which is not otherwise possible in the 2D monitoring of cardiomyocytes in monolayer.

3.1.3. Soft electrodes

Cardiomyocytes have contractile movements of contraction and relaxation. The cell-electrode interface is critical for enhanced extracellular recording, particularly for cardiomyocytes that have continuous movement. Thus, the mechanical property of the electrode material [122–124] must be considered to minimize the hindrance of cellular motion. Soft electrodes made of hydrogels and extremely thin materials [125] can significantly decrease the physical stress applied to the beating cells.

Liu et al. have developed a soft 3D electrode array to record the electrophysiology of cardiomyocytes [126] (Fig. 4i top). The highly conductive and tissue-like 3D electrode is made of an ionic liquid hydrogel mixed with PEDOT:PSS, then electrochemically deposited with iridium oxide. As it is made of hydrogel, the 3D micropillar electrode swells anisotropically in- and out-of-plane direction (Fig. 4i bottom). The height of the hydrogel micropillar can be increased from 1.8 μm and approximately up to 12.9 μm during swelling in PBS. The electrophysiological signals of the cardiomyocytes are measured with both the soft 3D electrode and the conventional rigid micropillar electrode. The soft 3D electrode records signals with a higher amplitude than the conventional rigid 3D electrode (Fig. 4j). Although the mechanical property of flexible MEAs is similar to that of the soft cells, nanoscale environment of the electrode-cell interface is significantly different compared to the intrinsically soft material like hydrogel. Also, the softness of the electrode improves the stability of the measurement, as the electrode can be bent along with the contraction-relaxation movement of the cardiomyocytes. Thus, the utilization of hydrogel as an electrode material is suitable for monitoring such constantly deforming cells like cardiomyocyte even if the intrinsic impedance of inorganic materials is much lower.

Recently, Lee et al. have reported ultrasoft nanomesh electrodes that conformally contact with the cardiomyocyte-hydrogel construct [127] (Fig. 4k top). The nanomesh device is fabricated out of electrospun polyurethane nanofibers, which are coated with gold and passivated with a parylene layer (Fig. 4k bottom). Due to the spaghetti-like structure, the nanomesh shows a high stretchability and extreme softness, and the beating motion of the cell is not hindered. Au-coated nanofibers are entangled together to create an electrical path which acts as an electrode. The nanomesh is extremely thin and contains a rough surface so that it can be tightly adhered onto the soft scaffold to achieve an enhanced quality of the electrode-cell interface. The electrical propagation of the cardiomyocytes can be recorded (Fig. 4l) without significant degradation of the device or damage to the cells due to the conformal adhesion of the highly stretchable nanomesh device onto the fibrin hydrogel seeded with the human induced pluripotent stem cell-derived cardiomyocytes (Fig. 4l inset).

3.1.4. Nanomaterial-based transistors

One of the main concerns in the development of heart-on-a-chip is to enhance signal quality and to accurately record electrical potentials of cardiomyocytes in detailed regions. Although passive MEAs are frequently used and have shown advances in recording extracellular cardiac signals, active MEAs [109,128], such as those integrated with field effect transistors, have been highlighted based on their several distinct features. One of their main advantages is that a higher density of recording sites integrated with the multiplexer [129,130] can be achieved. Also, the physical size of the recording region can be reduced dramatically. To improve the recording signal strength, nanomaterials such as nanowire are utilized in the field effect transistor. While the signal of hundreds of micro-volt can be recorded with passive MEAs, the nanowire FET can record the signals in the milli-volt range.

Dai et al. have demonstrated a 3D nanoelectronic array that can be folded easily to form a four-stacked device and recorded the 3D real-time mapping of extracellular cardiac action potentials [131] (Fig. 4m). Simply folding the flexible FET array multiple times allowed the 3D multilayer recording of the cardiomyocytes. The recording sites are made of FETs integrated with silicon nanowires and encapsulated with SU-8 polymer. A scaffold made of electrospun poly (lactic-co-glycolic acid) nanofibers is integrated at each layer of the sensor array of the 4×4 FET sensors. Also, the 3D propagation of the cardiac electrical potential is recorded in real time with an *in vitro* cardiac model. The flexible nanowire-integrated FET array enables the 3D spatiotemporal recording of the cardiac action potentials (Fig. 4n).

The organic electrochemical transistor (OECT) is another type of the transistor-based heart-on-a-chip. OECTs have attracted attention for their intrinsic flexibility and the high biocompatibility of the organic active layer [132], which is in direct contact with the cells [133–135]. Liang et al. have developed a flexible OECT to record cardiac action potentials *in vitro* [136]. A sub-micrometer thick layer of the conductive polymer, *i.e.*, PEDOT:PSS, is used as the channel material, leading to the fast exchange of ion charges between electrolytes and the channel (Fig. 4o top). Also, the recording performance of the OECT array is stable even under external strains (Fig. 4o bottom). HL-1 cardiac cells are cultured on the OECT array to record the propagation of the extracellular cardiac action potentials (Fig. 4p).

3.2. Electrodes for intracellular action potential measurement

The intracellular recording of cardiac action potentials offers tremendous information on cardiomyocytes such as the full amplitude and shape of the signal and activity of the ion channels in the cell membrane [137]. Although there is a possibility of damage to cell membranes, intracellular recording provides significantly more accurate recording data than extracellular recording. Thus, intracellular recording may be well suited to heart-on-a-chip and can be utilized specifically for screening drug-induced cardiotoxicity. Patch clamp electrodes [89] have been widely used to record the potential at the transmembrane by directly inserting the electrode into the cell [138] (Fig. 5a; inset for microscopic image of patch clamp). This technique is a common method and is considered as the gold standard due to its high signal-to-noise ratio and the reliability of the signal produced. It can even record the depolarization of the resting potential in cardiomyocytes that are treated with Na^+/K^+ pump inhibitor such as ouabain [88] (Fig. 5b). However, the patch clamp technique is unsuitable for long-term measurements due to its invasiveness. In addition, it cannot be applied as pharmacological screening platform due to its poor scalability.

3.2.1. Intracellular 3D recording electrodes

Various forms of vertical electrodes [91,139] have been demonstrated to record intracellular electrical potential of cardiac cells to overcome the drawbacks of the patch clamp technique. These vertical electrodes are usually made of 3D nanoelectrodes with a very thin and sharp structure, thereby creating a tight interface [140] between the cell membrane and the electrode [90]. Xie et al. have developed a nanopillar MEA to record the intracellular action potentials with an excellent signal strength for long period of time [141]. The nanopillar electrode with a length of 1.5 μm and a diameter of 150 nm is made of platinum and encapsulated with silicon nitride (Fig. 5c left). HL-1 cardiac cells are cultured on top of the nanopillar electrode, which is eventually engulfed tightly by the cell membrane (Fig. 5c right). Nevertheless, the electrode does not penetrate into the cells until high electric field is applied. Electroporation, which is widely used for inserting DNA into cells, can form nanometer-sized pores in the cell membrane with a very small voltage (Fig. 5d top). An electroporation increases the permeability of the cell, thereby leading to a dramatic increase in the signal amplitude by a factor of more than 100 (Fig. 5d bottom). However, the pore in the cell membrane by the electroporation seals back within several minutes. Thus, electroporation is needed each time during intracellular recording.

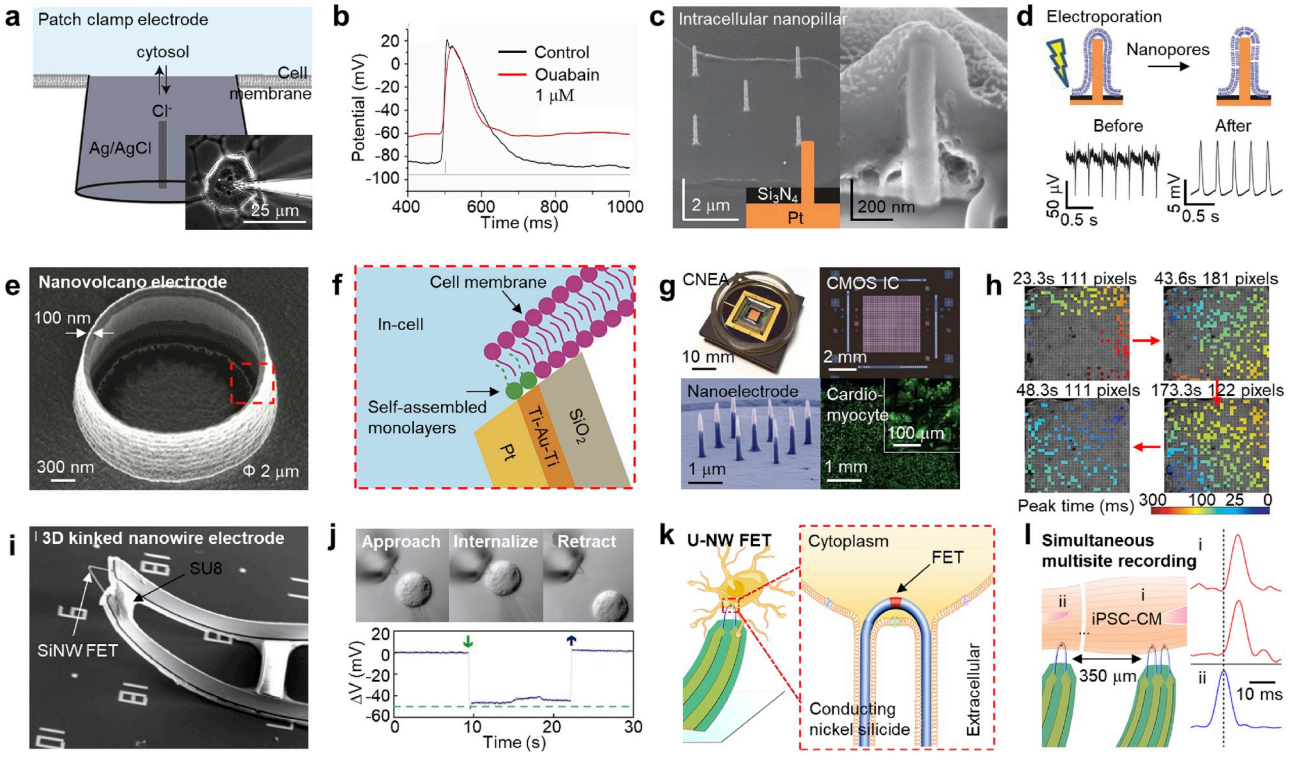

Fig. 5. Intracellular action potential recording. a) Schematic illustration of intracellular patch clamp electrode and SEM image of the patch clamp penetrated into cell (inset). Reprinted with permission [89,138]. Copyright 2015 Elsevier, Copyright 2009 Sage. b) Plot of cardiac action potential treated with an inhibitor of Na^+/K^+ pump, ouabain, recorded by patch clamp electrode. Reprinted with permission [88]. Copyright 2019 Elsevier. c) SEM image of intracellular nanopillar electrode (left) with an illustration showing the electrode material (inset) and close up image of the single nanopillar engulfed by the cell membrane (right). d) Schematic illustration of the nanopillar and cell membrane (top) and the recorded signals (bottom) before and after the electroporation. Reprinted with permission [141]. Copyright 2012 Nature Publishing Group. e) SEM image of a volcano-shaped nanopillar electrode with a diameter of 2 μm and thickness of 100 nm. f) Schematic illustration focused onto the electrode-cell interface (red-dotted box in Fig. 5e) showing the materials and layout. Reprinted with permission [142]. Copyright 2019 American Chemical Society. g) CMOS integrated nanopillar MEA. Images of device and its detailed configuration are shown starting from the whole image (top left), electrode array (top right), and nanopillars in single electrode (bottom left) to cultured cells (bottom right). h) Heat map of signal propagation into the clockwise direction by recording the intracellular action potential from thousands of electrodes. Reprinted with permission [147]. Copyright 2017 Nature Publishing Group. i) Microscope image of silicon nanowired FET cantilever. j) Microscope images showing the process of nanowire penetration into cellular membrane to record intracellular action potentials (top) and recorded signals (bottom). The arrows indicate the sensor at the contact (green) and detachment (purple) of cell membrane, respectively. Reprinted with permission [151]. Copyright 2010 American Association for the Advancement of Science. k) Schematic illustration of a U-shaped silicon nanowire FET cantilever (left) and the magnified view of the FET-cell interface (right). l) Schematic illustrations of two adjacent cardiomyocytes (i and ii cells) recorded by a paired U-shaped FET and single U-shaped FET (left), and the recorded data of intracellular signal time delay between the cells of i and ii (right). Reprinted with permission [152]. Copyright 2019 Nature Publishing Group. (For interpretation of the references to color in this figure legend, the reader is referred to the Web version of this article.)

For the long-term measurement of intracellular action potentials, Desbiolles et al. have demonstrated a volcano-shaped nano-patterned electrode (nano-volcano) that enables its passive insertion into the cell membrane with long-term stability of the cell-electrode interface [142]. The opening of the nano-volcano has a diameter of 2 μm (Fig. 5e), in which a small region of the cell can be captured. The electrode consists of an intracellular electrode made of a platinum and silicon oxide coating on the outside and a gold layer in-between for the attachment of self-assembled monolayers to improve the cell-electrode interface (Fig. 5f). Similar to the well-shaped electrode for extracellular potential recording, this nano-volcano electrode can greatly increase the surface area of the electrode-cell interface thereby decreasing the impedance at the sensing region. Also, the passive intracellular access allows the continuous recordings for up to 1 h which is much longer than the recording *via* electroporation.

The action potential of single cardiomyocyte is important; therefore, most methods focus on this measurement [143–145]. However, macroscopic information on the electrical activity of the entire cardiomyocytes in culture is also highly important to understanding drug-induced cardiotoxicity *in vitro* [146]. The cardiac action potential of single cardiomyocyte is propagated to the adjacent cells. Thus, the highly dense array of intracellular electrodes enables the extremely precise and parallel recordings of the cardiac cell network. Abbott et al. have reported on a high density array of 1026 intracellular recording electrodes integrated with complementary metal-oxide-semiconductor circuits [147] (CMOS; Fig. 5g top left). Among many previous researches for intracellular recording electrodes that have focused on materials and electrode designs for the improved electrode-cell interfacing, the development of a CMOS nanoelectrode array (CNEA) is highlighted in terms of its integration with CMOS and the recording of the cardiomyocyte activity with extremely high spatial resolution. The CNEA consists of 32 × 32 pixels (Fig. 5g top right) with nine nanoelectrodes made of platinum in each pixel (Fig. 5g bottom left). Also, each pixel is integrated with an amplifier to amplify the signals, and can switch the operation between recording and stimulation for electroporation. The neonatal rat ventricular cardiomyocytes are cultured on the device (Fig. 5g bottom right), and their action potentials are recorded by 1026 electrodes with an extremely high spatial resolution. Before electroporation, the heat map of the extracellular recording shows the homogeneous electrical propagation. After electroporation, a spiral map of intracellular electrical propagation is recorded (Fig. 5h). Also, the CNEA has been utilized as a drug screening platform to record cardiac dynamics such as beating frequency and conductance velocity after the treatment with norepinephrine and 1-heptanol on

cardiomyocytes.

3.2.2. Nanowire-based field effect transistors

Along with many advantages of nanowire-based FETs [148–150] (*e.g.*, high signal-to-noise ratio, minute physical size, and high density), another significant feature of the FETs is that their recording performance is independent to impedance. Several intracellular recording electrodes are designed as vertical 3D electrodes to form a tight interface between the cell membrane and electrode. However, FET-based probes are mostly used for extracellular recordings because they are fabricated on planar substrates.

Tian et al. however have developed 3D FET bioprobes integrated with silicon nanowires [151] (nanoFET) that are protruded upward into 3D space. Because the FET probe is not on a planar surface, these 3D nanoFETs enable the minimally invasive insertion of nanowire probes into the cell membrane for intracellular recordings. While there is a source, a drain, and channel within nanowire FETs, they are designed to form a kink with a sharp point in the 3D space (Fig. 5i). In the course of approach, internalize, and retract processes (Fig. 5j top), the nanoFETs have successfully recorded the electrical signals of single HL-1 cardiac cell (Fig. 5j bottom). As the active sensing area is made of extremely small nanowire, the nanoFET can enter the cells *via* an endocytic pathway similar to the introduction mechanism of nanoparticles. Nevertheless, there is a possibility that the cell membrane can be somewhat damaged by the insertion of the kinked nanowire.

Zhao et al. have advanced nanowire-based FET technology by controlling the design of silicon nanowire [152]. The nanowire is fabricated into a u-shape with a controlled length of the channel at the tip and enable intracellular recording (Fig. 5k). Although the number of the recording site is not comparable to other devices such as the MEA integrated with CMOS, the scalability of the device can be increased to six device regions containing 135 working FETs. Also, the U-shaped nanoFETs have enabled to record the full amplitude of the cardiac action potential, which is similar to the amplitude obtained by the patch clamp technique. Additionally, the U-shaped nanoFETs have demonstrated the recording of the signal propagation between two adjacent cardiac cells (Fig. 5l left). Human induced pluripotent stem cell-derived cardiomyocytes have been recorded with a pair of the U-shaped nanoFETs and another single nanoFET in the adjacent cells. Within the two channels of a pair of nanoFETs, no significant time delay in the signals is observed. But, the delay time of 6 ms between the single FET and a pair FETs in another cell (Fig. 5l right) agrees with the signal propagation speed reported in a previous study [153].

4. Conclusion

The desire to establish efficient and effective heart-on-a-chip for screening the toxicity of drug candidates in pharmacology has propelled the advancement in various devices for monitoring cardiomyocytes' behaviors. The ultimate goals of heart-on-a-chip is to emulate native heart tissue in an *in vitro* platform with accurate and fast monitoring capabilities. Also, simultaneous screening with massive scale in testing counts is needed to reduce the time and costs of drug discovery and to ascertain drug-related cardiotoxicity. Numerous studies on heart-on-a-chip have focused on mainly two different sensing modes: the physical contractility and the cardiac action potential. Thanks to the high sensitivity of light-based signals for recording cardiac contractility, optical-measurement-based sensing (*e.g.*, direct and calcium imaging and fluorescent, laser-based, and colorimetric sensing) enables a high-speed, accurate, and versatile monitoring of cardiac contractility. And, the electrical-signal-based sensors (*e.g.*, impedance sensor and strain gauge) integrated on thin film and flexible elastomer such as cantilever have achieved real-time and long-term recording of cardiac contractility.

In addition, the extracellular and intracellular cardiac action potentials are other prominent indicators of the condition of cardiomyocytes. Advancement in electrode design and materials, as well as the integration of flexible and soft bioelectronics in heart-on-a-chip, has been made to record the high-quality and high-density electrophysiological signals of the cardiomyocytes. Recording electrodes have been designed as MEAs both in planar and 3D form to increase the density of monitoring and to enhance cardiac signal strength. To increase the biocompatibility of electrode, carbon-based nanomaterials (*e.g.*, graphene and CNT) and organic conductive polymers (*e.g.*, PEDOT:PSS) have been utilized as electrode materials. In addition, a number of studies have focused on materials, such as silicon nanowire, and advanced fabrication techniques in intracellular electrodes to amplify recording signals up to the signals obtained from the patch clamp technique, while reducing damage to cell membranes by implementing soft and biocompatible materials. Recent developments in flexible and soft electronic technologies have enhanced the compatibility of *in vitro* platforms to native-mimicked cell environments such as engineered scaffold and 3D multicellular assembly.

Nevertheless, there are still challenges remain to achieve the current monitoring systems of contractility and cardiac action potentials. The optical-based measurements of cardiac contractility are difficult to perform simultaneous multiple recordings, while drug screening requires numerous repeated tests. Although the electrical sensing of cardiac contractions enables the real-time measurements, the number of recording sites and the capacity to process a large amount of data need further improvements. Thus, the deep learning technology of artificial intelligence (AI) can potentially be integrated with the sensors of heart-on-a-chip for both optical and electrical-based measurements to facilitate automated analysis and to improve the accuracy of cardiac physical and electrical monitoring. The physical characteristics (*e.g.*, size, shape, motility, moving patterns) and electrophysiological properties (*e.g.*, strength, velocity, and propagation pattern of action potential) of numerous cells can be acquired and analyzed by the integrated AI in order to ascertain both therapeutic and unexpected side effects of novel drug candidates and even increase the prediction capability to find new drugs [154,155]. In addition, intracellular recording systems that can achieve high-quality signal recording with high spatiotemporal resolution in the bio-mimicked 3D environment of scaffold remain limited. Further investigation into biocompatible nanomaterials and novel fabrication techniques to provide action potential recording of 3D cultured cardiomyocytes should be proceeded continuously, thereby, to establish a new gold standard for the efficient, precise, and long-term *in vitro* platforms for screening cardiotoxicity of drugs.

Author statement

Kyoung Won Cho: Conceptualization, Visualization, Writing - review & editing. Wang Hee Lee: Conceptualization, Visualization, Writing - review & editing. Byung-Soo Kim: Writing - review & editing. Dae-Hyeong Kim: Project administration, Supervision, Writing - review & editing.

Declaration of competing interest

The authors declare that they have no known competing financial interests or personal relationships that could have appeared to influence the work reported in this paper.

Acknowledgments

This work was supported by Institute for Basic Science (IBS-R006-A1), Republic of Korea.

References

[1] K. Hirose, A.Y. Payumo, S. Cutie, A. Hoang, H. Zhang, R. Guyot, D. Lunn, R.B. Bigley, H. Yu, J. Wang, M. Smith, E. Gillett, S.E. Muroy, T. Schmid, E. Wilson,

K.A. Field, D.M. Reeder, M. Maden, M.M. Yartsev, M.J. Wolfgang, F. Grützner, T.S. Scanlan, L.I. Szweda, R. Buffenstein, G. Hu, F. Flamant, J.E. Olgin, G.N. Huang, Evidence for hormonal control of heart regenerative capacity during endothermy acquisition, Science (2019) 80–364 eaar2038.
[2] W. Whyte, E.T. Roche, C.E. Varela, K. Mendez, S. Islam, H. O'Neill, F. Weafer, R.N. Shirazi, J.C. Weaver, N.V. Vasilyev, P.E. McHugh, B. Murphy, G.P. Duffy, C.J. Walsh, D.J. Mooney, Sustained release of targeted cardiac therapy with a replenishable implanted epicardial reservoir, Nat. Biomed. Eng. 2 (2018) 416–428.
[3] B.C. Schroeder, S. Waldegger, S. Fehr, M. Bleich, R. Warth, R. Greger, T.J. Jentsch, A constitutively open potassium channel formed by KCNQ1 and KCNE3, Nature 403 (2000) 196–199.
[4] A. Mathur, P. Loskill, K. Shao, N. Huebsch, S. Hong, S.G. Marcus, N. Marks, M. Mandegar, B.R. Conklin, L.P. Lee, K.E. Healy, Human iPSC-based cardiac microphysiological system for drug screening applications, Sci. Rep. 5 (2015) 8883.
[5] H. Savoji, M.H. Mohammadi, N. Rafatian, M.K. Toroghi, E.Y. Wang, Y. Zhao, A. Korolj, S. Ahadian, M. Radisic, Cardiovascular disease models: a game changing paradigm in drug discovery and screening, Biomaterials 198 (2019) 3–26.
[6] C.J. Torrance, V. Agrawal, B. Vogelstein, K.W. Kinzler, Use of isogenic human cancer cells for high-throughput screening and drug discovery, Nat. Biotechnol. 19 (2001) 940–945.
[7] K.W. Cho, S.J. Kim, J. Kim, S.Y. Song, W.H. Lee, L. Wang, M. Soh, N. Lu, T. Hyeon, B.-S. Kim, D.-H. Kim, Large scale and integrated platform for digital mass culture of anchorage dependent cells, Nat. Commun. 10 (2019) 4824.
[8] X. Zeng, J. Sun, S. Li, J. Shi, H. Gao, W. Sun Leong, Y. Wu, M. Li, C. Liu, P. Li, J. Kong, Y.-Z. Wu, G. Nie, Y. Fu, G. Zhang, Blood-triggered generation of platinum nanoparticle functions as an anti-cancer agent, Nat. Commun. 11 (2020) 567.
[9] J. Park, S. Choi, A.H. Janardhan, S.-Y. Lee, S. Raut, J. Soares, K. Shin, S. Yang, C. Lee, K.-W. Kang, H.R. Cho, S.J. Kim, P. Seo, W. Hyun, S. Jung, H.-J. Lee, N. Lee, S.H. Choi, M. Sacks, N. Lu, M.E. Josephson, T. Hyeon, D.-H. Kim, H.J. Hwang, Electromechanical cardioplasty using a wrapped elasto-conductive epicardial mesh, Sci. Transl. Med. 8 (2016) 344ra86-344ra86.
[10] J. Viventi, D.-H. Kim, J.D. Moss, Y.-S. Kim, J.A. Blanco, N. Annetta, A. Hicks, J. Xiao, Y. Huang, D.J. Callans, J.A. Rogers, B. Litt, A. Conformal, Bio-interfaced class of silicon electronics for mapping cardiac electrophysiology, Sci. Transl. Med. 2 (2010) 24ra22-24ra22.
[11] S. Sunwoo, S.I. Han, H. Kang, Y.S. Cho, D. Jung, C. Lim, C. Lim, M. Cha, S. Lee, T. Hyeon, D. Kim, Stretchable low-impedance nanocomposite comprised of Ag–Au core–shell nanowires and Pt black for epicardial recording and stimulation, Adv. Mater. Technol. 5 (2020) 1900768.
[12] D.H. Kim, R. Ghaffari, N. Lu, S. Wang, S.P. Lee, H. Keum, R. D'Angelo, L. Klinker, Y. Su, C. Lu, Y.S. Kim, A. Ameen, Y. Li, Y. Zhang, B. De Graff, Y.Y. Hsu, Z.J. Liu, J. Ruskin, L. Xu, C. Lu, F.G. Omenetto, Y. Huang, M. Mansour, M.J. Slepian, J.A. Rogers, Electronic sensor and actuator webs for large-area complex geometry cardiac mapping and therapy, Proc. Natl. Acad. Sci. U. S. A 109 (2012) 19910–19915.
[13] J. Li, D.J. Mooney, Designing hydrogels for controlled drug delivery, Nat. Rev. Mater. 1 (2016).
[14] E. Lounkine, M.J. Keiser, S. Whitebread, D. Mikhailov, J. Hamon, J.L. Jenkins, P. Lavan, E. Weber, A.K. Doak, S. Côté, B.K. Shoichet, L. Urban, Large-scale prediction and testing of drug activity on side-effect targets, Nature 486 (2012) 361–367.
[15] M. Sirota, J.T. Dudley, J. Kim, A.P. Chiang, A.A. Morgan, A. Sweet-Cordero, J. Sage, A.J. Butte, Discovery and preclinical validation of drug indications using compendia of public gene expression data, Sci. Transl. Med. 3 (2011) 96ra77-96ra77.
[16] S.U. Vorrink, Y. Zhou, M. Ingelman-Sundberg, V.M. Lauschke, Prediction of drug-induced hepatotoxicity using long-term stable primary hepatic 3D spheroid cultures in chemically defined conditions, Toxicol. Sci. 163 (2018) 655–665.
[17] D. Huh, D.C. Leslie, B.D. Matthews, J.P. Fraser, S. Jurek, G.A. Hamilton, K.S. Thorneloe, M.A. McAlexander, D.E. Ingber, A human disease model of drug toxicity–induced pulmonary edema in a lung-on-a-chip microdevice, Sci. Transl. Med. 4 (2012) 159ra147-159ra147.
[18] S.J. Kim, K.W. Cho, H.R. Cho, L. Wang, S.Y. Park, S.E. Lee, T. Hyeon, N. Lu, S.H. Choi, D.-H. Kim, Stretchable and transparent biointerface using cell-sheet-graphene hybrid for electrophysiology and therapy of skeletal muscle, Adv. Funct. Mater. 26 (2016) 3207–3217.
[19] V. Shinde, P. Sureshkumar, I. Sotiriadou, J. Hescheler, A. Sachinidis, Human embryonic and induced pluripotent stem cell based toxicity testing models: future applications in new drug discovery, Curr. Med. Chem. 23 (2016) 3495–3509.
[20] S.O. Mueller, W. Dekant, P. Jennings, E. Testai, F. Bois, Comprehensive summary – predict-IV: a systems toxicology approach to improve pharmaceutical drug safety testing, Toxicol. Vitro 30 (2015) 4–6.
[21] D.B. Fogel, Factors associated with clinical trials that fail and opportunities for improving the likelihood of success: a review, Contemp. Clin. Trials Commun. 11 (2018) 156–164.
[22] J. Bailey, M. Balls, Recent efforts to elucidate the scientific validity of animal-based drug tests by the pharmaceutical industry, pro-testing lobby groups, and animal welfare organisations, BMC Med. Ethics 20 (2019) 1–7.
[23] O. Hurko, J.L. Ryan, Translational research in central nervous system drug discovery, NeuroRx 2 (2005) 671–682.
[24] K.-J. Jang, M.A. Otieno, J. Ronxhi, H.-K. Lim, L. Ewart, K.R. Kodella, D.B. Petropolis, G. Kulkarni, J.E. Rubins, D. Conegliano, J. Nawroth, D. Simic, W. Lam, M. Singer, E. Barale, B. Singh, M. Sonee, A.J. Streeter, C. Manthey, B. Jones, A. Srivastava, L.C. Andersson, D. Williams, H. Park, R. Barrile, J. Sliz, A. Herland, S. Haney, K. Karalis, D.E. Ingber, G.A. Hamilton, Reproducing human and cross-species drug toxicities using a Liver-Chip, Sci. Transl. Med. 11 (2019) eaax5516.
[25] N.M. Mordwinkin, P.W. Burridge, J.C. Wu, A review of human pluripotent stem cell-derived cardiomyocytes for high-throughput drug discovery, cardiotoxicity screening, and publication standards, J. Cardiovasc. Transl. Res. 6 (2013) 22–30.
[26] J.H. Song, S.M. Lee, K.H. Yoo, Label-free and real-time monitoring of human mesenchymal stem cell differentiation in 2D and 3D cell culture systems using impedance cell sensors, RSC Adv. 8 (2018) 31246–31254.
[27] H. Wan, C. Gu, Y. Gan, X. Wei, K. Zhu, N. Hu, P. Wang, Sensor-free and sensor-based heart-on-a-chip platform: a review of design and applications, Curr. Pharmaceut. Des. 24 (2019) 5375–5385.
[28] J. Kieninger, A. Weltin, H. Flamm, G.A. Urban, Microsensor systems for cell metabolism-from 2D culture to organ-on-chip, Lab Chip 18 (2018) 1274–1291.
[29] E.W. Esch, A. Bahinski, D. Huh, Organs-on-chips at the frontiers of drug discovery, Nat. Rev. Drug Discov. 14 (2015) 248–260.
[30] R. Novak, M. Ingram, S. Marquez, D. Das, A. Delahanty, A. Herland, B.M. Maoz, S.S.F. Jeanty, M.R. Somayaji, M. Burt, E. Calamari, A. Chalkiadaki, A. Cho, Y. Choe, D.B. Chou, M. Cronce, S. Dauth, T. Divic, J. Fernandez-Alcon, T. Ferrante, J. Ferrier, E.A. FitzGerald, R. Fleming, S. Jalili-Firoozinezhad, T. Grevesse, J.A. Goss, T. Hamkins-Indik, O. Henry, C. Hinojosa, T. Huffstater, K.-J. Jang, V. Kujala, L. Leng, R. Mannix, Y. Milton, J. Nawroth, B.A. Nestor, C.F. Ng, B. O'Connor, T.-E. Park, H. Sanchez, J. Sliz, A. Sontheimer-Phelps, B. Swenor, G. Thompson, G.J. Touloumes, Z. Tranchemontagne, N. Wen, M. Yadid, A. Bahinski, G.A. Hamilton, D. Levner, O. Levy, A. Przekwas, R. Prantil-Baun, K.K. Parker, D.E. Ingber, Robotic fluidic coupling and interrogation of multiple vascularized organ chips, Nat. Biomed. Eng. 4 (2020) 407–420.
[31] T.-E. Park, N. Mustafaoglu, A. Herland, R. Hasselkus, R. Mannix, E.A. FitzGerald, R. Prantil-Baun, A. Watters, O. Henry, M. Benz, H. Sanchez, H.J. McCrea, L.C. Goumnerova, H.W. Song, S.P. Palecek, E. Shusta, D.E. Ingber, Hypoxia-enhanced Blood-Brain Barrier Chip recapitulates human barrier function and shuttling of drugs and antibodies, Nat. Commun. 10 (2019) 2621.
[32] D. Huh, B.D. Matthews, A. Mammoto, M. Montoya-Zavala, H.Y. Hsin, D.E. Ingber, Reconstituting organ-level lung functions on a chip, Science 328 (2010) 1662–1668 80-.
[33] E. Jastrzebska, E. Tomecka, I. Jesion, Heart-on-a-chip based on stem cell biology, Biosens. Bioelectron. 75 (2016) 67–81.
[34] S. Hong, J. Lee, K. Do, M. Lee, J.H. Kim, S. Lee, D.-H. Kim, Stretchable electrode based on laterally combed carbon nanotubes for wearable energy harvesting and storage devices, Adv. Funct. Mater. 27 (2017) 1704353.
[35] J. Han, Y.S. Kim, M.Y. Lim, H.Y. Kim, S. Kong, M. Kang, Y.W. Choo, J.H. Jun, S. Ryu, H.Y. Jeong, J. Park, G.J. Jeong, J.C. Lee, G.H. Eom, Y. Ahn, B.S. Kim, Dual roles of graphene oxide to attenuate inflammation and elicit timely polarization of macrophage phenotypes for cardiac repair, ACS Nano 12 (2018) 1959–1977.
[36] P.Y. Mengsteab, K. Uto, A.S.T. Smith, S. Frankel, E. Fisher, Z. Nawas, J. Macadangdang, M. Ebara, D.-H. Kim, Spatiotemporal control of cardiac anisotropy using dynamic nanotopographic cues, Biomaterials 86 (2016) 1–10.
[37] J.H. Tsui, N.A. Ostrovsky-Snider, D.M.P. Yama, J.D. Donohue, J.S. Choi, R. Chavanachat, J.D. Larson, A.R. Murphy, D.-H. Kim, Conductive silk–polypyrrole composite scaffolds with bioinspired nanotopographic cues for cardiac tissue engineering, J. Mater. Chem. B. 6 (2018) 7185–7196.
[38] C. Choi, M.K. Choi, S. Liu, M.S. Kim, O.K. Park, C. Im, J. Kim, X. Qin, G.J. Lee, K.W. Cho, M. Kim, E. Joh, J. Lee, D. Son, S.-H. Kwon, N.L. Jeon, Y.M. Song, N. Lu, D.-H. Kim, Human eye-inspired soft optoelectronic device using high-density MoS2-graphene curved image sensor array, Nat. Commun. 8 (2017) 1664.
[39] J. Kim, M. Lee, H.J. Shim, R. Ghaffari, H.R. Cho, D. Son, Y.H. Jung, M. Soh, C. Choi, S. Jung, K. Chu, D. Jeon, S.-T. Lee, J.H. Kim, S.H. Choi, T. Hyeon, D.-H. Kim, Stretchable silicon nanoribbon electronics for skin prosthesis, Nat. Commun. 5 (2014) 5747.
[40] S.Y. Song, J. Yoo, S. Go, J. Hong, H.S. Sohn, J.-R. Lee, M. Kang, G.-J. Jeong, S. Ryu, S.H.L. Kim, N.S. Hwang, K. Char, B.-S. Kim, Cardiac-mimetic cell-culture system for direct cardiac reprogramming, Theranostics 9 (2019) 6734–6744.
[41] J.-K. Yoon, T. Il Lee, S.H. Bhang, J.-Y. Shin, J.-M. Myoung, B.-S. Kim, Stretchable piezoelectric substrate providing pulsatile mechanoelectric cues for cardiomyogenic differentiation of mesenchymal stem cells, ACS Appl. Mater. Interfaces 9 (2017) 22101–22111.
[42] A.K. Capulli, L.A. MacQueen, S.P. Sheehy, K.K. Parker, Fibrous scaffolds for building hearts and heart parts, Adv. Drug Deliv. Rev. 96 (2016) 83–102.
[43] J. Chal, Z. Al Tanoury, M. Hestin, B. Gobert, S. Aivio, A. Hick, T. Cherrier, A.P. Nesmith, K.K. Parker, O. Pourquié, Generation of human muscle fibers and satellite-like cells from human pluripotent stem cells in vitro, Nat. Protoc. 11 (2016) 1833–1850.
[44] M. Shin, O. Ishii, T. Sueda, J.P. Vacanti, Contractile cardiac grafts using a novel nanofibrous mesh, Biomaterials 25 (2004) 3717–3723.
[45] J. Kim, R. Ghaffari, D.H. Kim, The quest for miniaturized soft bioelectronic devices, Nat. Biomed. Eng. 1 (2017) 1–4.
[46] D. Son, J. Lee, D.J. Lee, R. Ghaffari, S. Yun, S.J. Kim, J.E. Lee, H.R. Cho, S. Yoon, S. Yang, S. Lee, S. Qiao, D. Ling, S. Shin, J.-K. Song, J. Kim, T. Kim, H. Lee, J. Kim, M. Soh, N. Lee, C.S. Hwang, S. Nam, N. Lu, T. Hyeon, S.H. Choi, D.-H. Kim, Bioresorbable electronic stent integrated with therapeutic nanoparticles for endovascular diseases, ACS Nano 9 (2015) 5937–5946.
[47] C. Choi, M.K. Choi, T. Hyeon, D.-H. Kim, Nanomaterial-based soft electronics for healthcare applications, ChemNanoMat 2 (2016) 1006–1017.
[48] A. Herland, B.M. Maoz, D. Das, M.R. Somayaji, R. Prantil-Baun, R. Novak, M. Cronce, T. Huffstater, S.S.F. Jeanty, M. Ingram, A. Chalkiadaki, D. Benson Chou, S. Marquez, A. Delahanty, S. Jalili-Firoozinezhad, Y. Milton, A. Sontheimer-Phelps, B. Swenor, O. Levy, K.K. Parker, A. Przekwas, D.E. Ingber, Quantitative

prediction of human pharmacokinetic responses to drugs via fluidically coupled vascularized organ chips, Nat. Biomed. Eng. 4 (2020) 421–436.
[49] A.J.S. Ribeiro, K. Zaleta-Rivera, E.A. Ashley, B.L. Pruitt, Stable, covalent attachment of laminin to microposts improves the contractility of mouse neonatal cardiomyocytes, ACS Appl. Mater. Interfaces 6 (2014) 15516–15526.
[50] T. Kaneko, E. Takizawa, F. Nomura, T. Hamada, A. Hattori, K. Yasuda, On-chip single-cell-shape control technology for understanding contractile motion of cardiomyocytes measured using optical image analysis system, Jpn. J. Appl. Phys. 52 (2013) 06GK06.
[51] S.J. Kim, H.R. Cho, K.W. Cho, S. Qiao, J.S. Rhim, M. Soh, T. Kim, M.K. Choi, C. Choi, I. Park, N.S. Hwang, T. Hyeon, S.H. Choi, N. Lu, D.H. Kim, Multifunctional cell-culture platform for aligned cell sheet monitoring, transfer printing, and therapy, ACS Nano 9 (2015) 2677–2688.
[52] C. Bazan, D.T. Barba, T. Hawkins, H. Nguyen, S. Anderson, E. Vazquez-Hidalgo, R. Lemus, J. Moore, J. Mitchell, J. Martinez, D. Moore, J. Larsen, P. Paolini, Contractility assessment in enzymatically isolated cardiomyocytes, Biophys. Rev. 4 (2012) 231–243.
[53] O. Sirenko, C. Crittenden, N. Callamaras, J. Hesley, Y.-W. Chen, C. Funes, I. Rusyn, B. Anson, E.F. Cromwell, Multiparameter in vitro assessment of compound effects on cardiomyocyte physiology using iPSC cells, J. Biomol. Screen 18 (2013) 39–53.
[54] K. Breckwoldt, D. Letuffe-Brenière, I. Mannhardt, T. Schulze, B. Ulmer, T. Werner, A. Benzin, B. Klampe, M.C. Reinsch, S. Laufer, A. Shibamiya, M. Prondzynski, G. Mearini, D. Schade, S. Fuchs, C. Neuber, E. Krämer, U. Saleem, M.L. Schulze, M.L. Rodriguez, T. Eschenhagen, A. Hansen, Differentiation of cardiomyocytes and generation of human engineered heart tissue, Nat. Protoc. 12 (2017) 1177–1197.
[55] A. Czirok, D.G. Isai, E. Kosa, S. Rajasingh, W. Kinsey, Z. Neufeld, J. Rajasingh, Optical-flow based non-invasive analysis of cardiomyocyte contractility, Sci. Rep. 7 (2017) 10404.
[56] E. Matsa, P.W. Burridge, J.C. Wu, Human stem cells for modeling heart disease and for drug discovery, Sci. Transl. Med. 6 (2014) 239ps6-239ps6.
[57] T. Meyer, M. Tiburcy, W.-H. Zimmermann, Cardiac macrotissues-on-a-plate models for phenotypic drug screens, Adv. Drug Deliv. Rev. 140 (2019) 93–100.
[58] L.M.D. Delbridge, K.P. Roos, Optical methods to evaluate the contractile function of unloaded isolated cardiac myocytes, J. Mol. Cell. Cardiol. 29 (1997) 11–25.
[59] A. Pointon, J. Pilling, T. Dorval, Y. Wang, C. Archer, C. Pollard, From the cover: high-throughput imaging of cardiac microtissues for the assessment of cardiac contraction during drug discovery, Toxicol. Sci. 155 (2017) 444–457.
[60] K.M. Beussman, M.L. Rodriguez, A. Leonard, N. Taparia, C.R. Thompson, N.J. Sniadecki, Micropost arrays for measuring stem cell-derived cardiomyocyte contractility, Methods 94 (2016) 43–50.
[61] H. Colin-York, M. Fritzsche, The future of traction force microscopy, Curr. Opin. Biomed. Eng. 5 (2018) 1–5.
[62] Z. Jian, H. Han, T. Zhang, J. Puglisi, L.T. Izu, J.A. Shaw, E. Onofiok, J.R. Erickson, Y.-J. Chen, B. Horvath, R. Shimkunas, W. Xiao, Y. Li, T. Pan, J. Chan, T. Banyasz, J.C. Tardiff, N. Chiamvimonvat, D.M. Bers, K.S. Lam, Y. Chen-Izu, Mechanochemotransduction during cardiomyocyte contraction is mediated by localized nitric oxide signaling, Sci. Signal. 7 (2014) ra27–ra27.
[63] N.-E. Oyunbaatar, Y. Dai, A. Shanmugasundaram, B.-K. Lee, E.-S. Kim, D.-W. Lee, Development of a next-generation biosensing platform for simultaneous detection of mechano- and electrophysiology of the drug-induced cardiomyocytes, ACS Sens. 4 (2019) 2623–2630.
[64] M. Pesl, J. Pribyl, I. Acimovic, A. Vilotic, S. Jelinkova, A. Salykin, A. Lacampagne, P. Dvorak, A.C. Meli, P. Skladal, V. Rotrekl, Atomic force microscopy combined with human pluripotent stem cell derived cardiomyocytes for biomechanical sensing, Biosens. Bioelectron. 85 (2016) 751–757.
[65] Y. Shang, Z. Chen, F. Fu, L. Sun, C. Shao, W. Jin, H. Liu, Y. Zhao, Cardiomyocyte-driven structural color actuation in anisotropic inverse opals, ACS Nano 13 (2019) 796–802.
[66] K.P. Roos, A.J. Brady, Individual sarcomere length determination from isolated cardiac cells using high-resolution optical microscopy and digital image processing, Biophys. J. 40 (1982) 233–244.
[67] L. Wang, W. Dou, M. Malhi, M. Zhu, H. Liu, J. Plakhotnik, Z. Xu, Q. Zhao, J. Chen, S. Chen, R. Hamilton, C.A. Simmons, J.T. Maynes, Y. Sun, Microdevice platform for continuous measurement of contractility, beating rate, and beating rhythm of human-induced pluripotent stem cell-cardiomyocytes inside a controlled incubator environment, ACS Appl. Mater. Interfaces 10 (2018) 21173–21183.
[68] A.J.S. Ribeiro, Y.-S. Ang, J.-D. Fu, R.N. Rivas, T.M.A. Mohamed, G.C. Higgs, D. Srivastava, B.L. Pruitt, Contractility of single cardiomyocytes differentiated from pluripotent stem cells depends on physiological shape and substrate stiffness, Proc. Natl. Acad. Sci. Unit. States Am. 112 (2015) 12705–12710.
[69] D.H. Kim, E.A. Lipke, P. Kim, R. Cheong, S. Thompson, M. Delannoy, K.Y. Suh, L. Tung, A. Levchenko, Nanoscale cues regulate the structure and function of macroscopic cardiac tissue constructs, Proc. Natl. Acad. Sci. U. S. A 107 (2010) 565–570.
[70] L. Gu, D.J. Hall, Z. Qin, E. Anglin, J. Joo, D.J. Mooney, S.B. Howell, M.J. Sailor, In vivo time-gated fluorescence imaging with biodegradable luminescent porous silicon nanoparticles, Nat. Commun. 4 (2013) 2326.
[71] H. Watanabe, Y. Honda, J. Deguchi, T. Yamada, K. Bando, Usefulness of cardiotoxicity assessment using calcium transient in human induced pluripotent stem cell-derived cardiomyocytes, J. Toxicol. Sci. 42 (2017) 519–527.
[72] S. Björk, E.A. Ojala, T. Nordström, A. Ahola, M. Liljeström, J. Hyttinen, E. Kankuri, E. Mervaala, Evaluation of optogenetic electrophysiology tools in human stem cell-derived cardiomyocytes, Front. Physiol. 8 (2017).
[73] S.-Y. Lee, D.-S. Kim, E.-S. Kim, D.-W. Lee, Nano-textured polyimide cantilever for enhancing the contractile behavior of cardiomyocytes and its application to cardiac toxicity screening, Sensor. Actuator. B Chem. 301 (2019) 126995.
[74] A. Gaitas, R. Malhotra, T. Li, T. Herron, J. Jalife, A device for rapid and quantitative measurement of cardiac myocyte contractility, Rev. Sci. Instrum. 86 (2015) 034302.
[75] L. Li, Z. Chen, C. Shao, L. Sun, L. Sun, Y. Zhao, Graphene hybrid anisotropic structural color film for cardiomyocytes' monitoring, Adv. Funct. Mater. 30 (2020) 1906353.
[76] S. Ahn, H.A.M. Ardoña, J.U. Lind, F. Eweje, S.L. Kim, G.M. Gonzalez, Q. Liu, J.F. Zimmerman, G. Pyrgiotakis, Z. Zhang, J. Beltran-Huarac, P. Carpinone, B.M. Moudgil, P. Demokritou, K.K. Parker, Mussel-inspired 3D fiber scaffolds for heart-on-a-chip toxicity studies of engineered nanomaterials, Anal. Bioanal. Chem. 410 (2018) 6141–6154.
[77] S. Choi, S.I. Han, D. Jung, H.J. Hwang, C. Lim, S. Bae, O.K. Park, C.M. Tschabrunn, M. Lee, S.Y. Bae, J.W. Yu, J.H. Ryu, S.-W. Lee, K. Park, P.M. Kang, W.B. Lee, R. Nezafat, T. Hyeon, D.-H. Kim, Highly conductive, stretchable and biocompatible Ag–Au core–sheath nanowire composite for wearable and implantable bioelectronics, Nat. Nanotechnol. 13 (2018) 1048–1056.
[78] F. Qian, C. Huang, Y.-D. Lin, A.N. Ivanovskaya, T.J. O'Hara, R.H. Booth, C.J. Creek, H.A. Enright, D.A. Soscia, A.M. Belle, R. Liao, F.C. Lightstone, K.S. Kulp, E.K. Wheeler, Simultaneous electrical recording of cardiac electrophysiology and contraction on chip, Lab Chip 17 (2017) 1732–1739.
[79] J. Lee, H.R. Cho, G.D. Cha, H. Seo, S. Lee, C.-K. Park, J.W. Kim, S. Qiao, L. Wang, D. Kang, T. Kang, T. Ichikawa, J. Kim, H. Lee, W. Lee, S. Kim, S.-T. Lee, N. Lu, T. Hyeon, S.H. Choi, D.-H. Kim, Flexible, sticky, and biodegradable wireless device for drug delivery to brain tumors, Nat. Commun. 10 (2019) 5205.
[80] A. Oláh, M. Ruppert, T.I. Orbán, Á. Apáti, B. Sarkadi, B. Merkely, T. Radovits, Hemodynamic characterization of a transgenic rat strain stably expressing the calcium sensor protein GCAMP2, Am. J. Physiol. Heart Circ. Physiol. 316 (2019) H1224–H1228.
[81] A.S. Cheung, D.K.Y. Zhang, S.T. Koshy, D.J. Mooney, Scaffolds that mimic antigen-presenting cells enable ex vivo expansion of primary T cells, Nat, Biotechnol. 36 (2018) 160–169.
[82] J.U. Lind, T.A. Busbee, A.D. Valentine, F.S. Pasqualini, H. Yuan, M. Yadid, S.-J. Park, A. Kotikian, A.P. Nesmith, P.H. Campbell, J.J. Vlassak, J.A. Lewis, K.K. Parker, Instrumented cardiac microphysiological devices via multimaterial three-dimensional printing, Nat. Mater. 16 (2017) 303–308.
[83] Y. Kim, H. Yuk, R. Zhao, S.A. Chester, X. Zhao, Printing ferromagnetic domains for untethered fast-transforming soft materials, Nature 558 (2018) 274–279.
[84] D.-S. Kim, Y.W. Choi, A. Shanmugasundaram, Y.-J. Jeong, J. Park, N.-E. Oyunbaatar, E.-S. Kim, M. Choi, D.-W. Lee, Highly durable crack sensor integrated with silicone rubber cantilever for measuring cardiac contractility, Nat. Commun. 11 (2020) 535.
[85] D.-H. Kim, R. Ghaffari, N. Lu, J.A. Rogers, Flexible and stretchable electronics for biointegrated devices, Annu. Rev. Biomed. Eng. 14 (2012) 113–128.
[86] D.H. Kim, J. Song, M.C. Won, H.S. Kim, R.H. Kim, Z. Liu, Y.Y. Huang, K.C. Hwang, Y.W. Zhang, J.A. Rogers, Materials and noncoplanar mesh designs for integrated circuits with linear elastic responses to extreme mechanical deformations, Proc. Natl. Acad. Sci. U. S. A 105 (2008) 18675–18680.
[87] D.C. Kim, H.J. Shim, W. Lee, J.H. Koo, D. Kim, Material-based approaches for the fabrication of stretchable electronics, Adv. Mater. 1902743 (2019) 1902743.
[88] S.A. Mann, J. Heide, T. Knott, R. Airini, F.B. Epureanu, A.-F. Deftu, A.-T. Deftu, B.M. Radu, B. Amuzescu, Recording of multiple ion current components and action potentials in human induced pluripotent stem cell-derived cardiomyocytes via automated patch-clamp, J. Pharmacol. Toxicol. Methods 100 (2019) 106599.
[89] N. Akanda, P. Molnar, M. Stancescu, J.J. Hickman, Analysis of toxin-induced changes in action potential shape for drug development, J. Biomol. Screen 14 (2009) 1228–1235.
[90] Z.C. Lin, A.F. McGuire, P.W. Burridge, E. Matsa, H.-Y. Lou, J.C. Wu, B. Cui, Accurate nanoelectrode recording of human pluripotent stem cell-derived cardiomyocytes for assaying drugs and modeling disease, Microsystems Nanoeng 3 (2017) 16080.
[91] M. Dipalo, H. Amin, L. Lovato, F. Moia, V. Caprettini, G.C. Messina, F. Tantussi, L. Berdondini, F. De Angelis, Intracellular and extracellular recording of spontaneous action potentials in mammalian neurons and cardiac cells with 3D plasmonic nanoelectrodes, Nano Lett. 17 (2017) 3932–3939.
[92] A. Alassaf, G. Tansik, V. Mayo, L. Wubker, D. Carbonero, A. Agarwal, Engineering anisotropic cardiac monolayers on microelectrode arrays for non-invasive analyses of electrophysiological properties, Analyst 145 (2020) 139–149.
[93] J.S. Park, S.I. Grijalva, D. Jung, S. Li, G.V. Junek, T. Chi, H.C. Cho, H. Wang, Intracellular cardiomyocytes potential recording by planar electrode array and fibroblasts co-culturing on multi-modal CMOS chip, Biosens. Bioelectron. 144 (2019) 111626.
[94] Y.J. Hong, H. Jeong, K.W. Cho, N. Lu, D.H. Kim, Wearable and implantable devices for cardiovascular healthcare: from monitoring to therapy based on flexible and stretchable electronics, Adv. Funct. Mater. 29 (2019) 1–26.
[95] J. Ren, Q. Xu, X. Chen, W. Li, K. Guo, Y. Zhao, Q. Wang, Z. Zhang, H. Peng, Y.-G. Li, Superaligned carbon nanotubes guide oriented cell growth and promote electrophysiological homogeneity for synthetic cardiac tissues, Adv. Mater. 29 (2017) 1702713.
[96] T. Weigel, T. Pfister, T. Schmitz, M. Jannasch, S. Schürlein, R. Al Hijailan, H. Walles, J. Hansmann, Flexible tissue-like electrode as a seamless tissue-electronic interface, BioNanoMaterials 18 (2017).
[97] M. Lee, H.J. Shim, C. Choi, D.H. Kim, Soft high-resolution neural interfacing probes: materials and design approaches, Nano Lett. 19 (2019) 2741–2749.
[98] T. Cohen-Karni, Q. Qing, Q. Li, Y. Fang, C.M. Lieber, Graphene and nanowire transistors for cellular interfaces and electrical recording, Nano Lett. 10 (2010) 1098–1102.

[99] J.H. Koo, S. Jeong, H.J. Shim, D. Son, J. Kim, D.C. Kim, S. Choi, J.I. Hong, D.H. Kim, Wearable electrocardiogram monitor using carbon nanotube electronics and color-tunable organic light-emitting diodes, ACS Nano 11 (2017) 10032–10041.

[100] C. Choi, Y. Lee, K.W. Cho, J.H. Koo, D.H. Kim, Wearable and implantable soft bioelectronics using two-dimensional materials, Acc. Chem. Res. 52 (2019) 73–81.

[101] H. Lee, Y. Lee, C. Song, H.R. Cho, R. Ghaffari, T.K. Choi, K.H. Kim, Y.B. Lee, D. Ling, H. Lee, S.J. Yu, S.H. Choi, T. Hyeon, D.H. Kim, An endoscope with integrated transparent bioelectronics and theranostic nanoparticles for colon cancer treatment, Nat. Commun. 6 (2015) 1–10.

[102] D. Kireev, S. Seyock, J. Lewen, V. Maybeck, B. Wolfrum, A. Offenhäusser, Graphene multielectrode arrays as a versatile tool for extracellular measurements, Adv. Healthc. Mater. 6 (2017) 1601433.

[103] T. Sharf, P.K. Hansma, M.A. Hari, K.S. Kosik, Non-contact monitoring of extracellular field potentials with a multi-electrode array, Lab Chip 19 (2019) 1448–1457.

[104] B.M. Maoz, A. Herland, O.Y.F. Henry, W.D. Leineweber, M. Yadid, J. Doyle, R. Mannix, V.J. Kujala, E.A. FitzGerald, K.K. Parker, D.E. Ingber, Organs-on-Chips with combined multi-electrode array and transepithelial electrical resistance measurement capabilities, Lab Chip 17 (2017) 2294–2302.

[105] N. Zhang, F. Stauffer, B.R. Simona, F. Zhang, Z.-M. Zhang, N.-P. Huang, J. Vörös, Multifunctional 3D electrode platform for real-time in situ monitoring and stimulation of cardiac tissues, Biosens. Bioelectron. 112 (2018) 149–155.

[106] J. Cools, D. Copic, Z. Luo, G. Callewaert, D. Braeken, M. De Volder, 3D microstructured carbon nanotube electrodes for trapping and recording electrogenic cells, Adv. Funct. Mater. 27 (2017) 1701083.

[107] A.S.T. Smith, E. Choi, K. Gray, J. Macadangdang, E.H. Ahn, E.C. Clark, M.A. Laflamme, J.C. Wu, C.E. Murry, L. Tung, D.H. Kim, NanoMEA: a tool for high-throughput, electrophysiological phenotyping of patterned excitable cells, Nano Lett. 20 (2020) 1561–1570.

[108] A.S.T. Smith, J. Macadangdang, W. Leung, M.A. Laflamme, D.-H. Kim, Human iPSC-derived cardiomyocytes and tissue engineering strategies for disease modeling and drug screening, Biotechnol. Adv. 35 (2017) 77–94.

[109] B. Tian, J. Liu, T. Dvir, L. Jin, J.H. Tsui, Q. Qing, Z. Suo, R. Langer, D.S. Kohane, C.M. Lieber, Macroporous nanowire nanoelectronic scaffolds for synthetic tissues, Nat. Mater. 11 (2012) 986–994.

[110] C.P. Soares, V. Midlej, M.E.W. de Oliveira, M. Benchimol, M.L. Costa, C. Mermelstein, 2D and 3D-organized cardiac cells shows differences in cellular morphology, adhesion junctions, presence of myofibrils and protein expression, PloS One 7 (2012).

[111] M. Shin, H. Yoshimoto, J.P. Vacanti, In vivo bone tissue engineering using mesenchymal stem cells on a novel electrospun nanofibrous scaffold, Tissue Eng. 10 (2004) 33–41.

[112] C. Mandrycky, Z. Wang, K. Kim, D.-H. Kim, 3D bioprinting for engineering complex tissues, Biotechnol. Adv. 34 (2016) 422–434.

[113] C. Lim, Y. Shin, J. Jung, J.H. Kim, S. Lee, D.H. Kim, Stretchable conductive nanocomposite based on alginate hydrogel and silver nanowires for wearable electronics, Apl. Mater. 7 (2019).

[114] Y.S. Zhang, J. Aleman, S.R. Shin, T. Kilic, D. Kim, S.A. Mousavi Shaegh, S. Massa, R. Riahi, S. Chae, N. Hu, H. Avci, W. Zhang, A. Silvestri, A. Sanati Nezhad, A. Manbohi, F. De Ferrari, A. Polini, G. Calzone, N. Shaikh, P. Alerasool, E. Budina, J. Kang, N. Bhise, J. Ribas, A. Pourmand, A. Skardal, T. Shupe, C.E. Bishop, M.R. Dokmeci, A. Atala, A. Khademhosseini, Multisensor-integrated organs-on-chips platform for automated and continual in situ monitoring of organoid behaviors, Proc. Natl. Acad. Sci. Unit. States Am. 114 (2017) E2293–E2302.

[115] J.-K. Song, D. Son, J. Kim, Y.J. Yoo, G.J. Lee, L. Wang, M.K. Choi, J. Yang, M. Lee, K. Do, J.H. Koo, N. Lu, J.H. Kim, T. Hyeon, Y.M. Song, D.-H. Kim, Wearable force touch sensor array using a flexible and transparent electrode, Adv. Funct. Mater. 27 (2017) 1605286.

[116] H. Joo, D. Jung, S. Sunwoo, J.H. Koo, D. Kim, Material design and fabrication strategies for stretchable metallic nanocomposites, Small 16 (2020) 1906270.

[117] D.H. Kim, N. Lu, Y. Huang, J.A. Rogers, Materials for stretchable electronics in bioinspired and biointegrated devices, MRS Bull. 37 (2012) 226–235.

[118] Y. Lee, J. Kim, J.H. Koo, T.H. Kim, D.H. Kim, Nanomaterials for bioelectronics and integrated medical systems, Kor. J. Chem. Eng. 35 (2018) 1–11.

[119] G.D. Cha, D. Kang, J. Lee, D.H. Kim, Bioresorbable electronic implants: history, materials, fabrication, devices, and clinical applications, Adv. Healthc. Mater. 8 (2019) 1–20.

[120] R. Feiner, L. Engel, S. Fleischer, M. Malki, I. Gal, A. Shapira, Y. Shacham-Diamand, T. Dvir, Engineered hybrid cardiac patches with multifunctional electronics for online monitoring and regulation of tissue function, Nat. Mater. 15 (2016) 679–685.

[121] A. Kalmykov, C. Huang, J. Bliley, D. Shiwarski, J. Tashman, A. Abdullah, S.K. Rastogi, S. Shukla, E. Mataev, A.W. Feinberg, K.J. Hsia, T. Cohen-Karni, Organ-on-e-chip: three-dimensional self-rolled biosensor array for electrical interrogations of human electrogenic spheroids, Sci. Adv. 5 (2019) eaax0729.

[122] D.-H. Kim, J. Viventi, J.J. Amsden, J. Xiao, L. Vigeland, Y.-S. Kim, J.A. Blanco, B. Panilaitis, E.S. Frechette, D. Contreras, D.L. Kaplan, F.G. Omenetto, Y. Huang, K.-C. Hwang, M.R. Zakin, B. Litt, J.A. Rogers, Dissolvable films of silk fibroin for ultrathin conformal bio-integrated electronics, Nat. Mater. 9 (2010) 511–517.

[123] S. Choi, S.I. Han, D. Kim, T. Hyeon, D.H. Kim, High-performance stretchable conductive nanocomposites: materials, processes, and device applications, Chem. Soc. Rev. 48 (2019) 1566–1595.

[124] Y. Lee, J. Kim, H. Joo, M.S. Raj, R. Ghaffari, D.H. Kim, Wearable sensing systems with mechanically soft assemblies of nanoscale materials, Adv. Mater. Technol. 2 (2017) 1–18.

[125] M. Kaltenbrunner, T. Sekitani, J. Reeder, T. Yokota, K. Kuribara, T. Tokuhara, M. Drack, R. Schwödiauer, I. Graz, S. Bauer-Gogonea, S. Bauer, T. Someya, An ultra-lightweight design for imperceptible plastic electronics, Nature 499 (2013) 458–463.

[126] Y. Liu, A.F. McGuire, H.-Y. Lou, T.L. Li, J.B.H. Tok, B. Cui, Z. Bao, Soft conductive micropillar electrode arrays for biologically relevant electrophysiological recording, Proc. Natl. Acad. Sci. Unit. States Am. 115 (2018) 11718–11723.

[127] S. Lee, D. Sasaki, D. Kim, M. Mori, T. Yokota, H. Lee, S. Park, K. Fukuda, M. Sekino, K. Matsuura, T. Shimizu, T. Someya, Ultrasoft electronics to monitor dynamically pulsing cardiomyocytes, Nat. Nanotechnol. 14 (2019) 156–160.

[128] M. Imboden, E. de Coulon, A. Poulin, C. Dellenbach, S. Rosset, H. Shea, S. Rohr, High-speed mechano-active multielectrode array for investigating rapid stretch effects on cardiac tissue, Nat. Commun. 10 (2019) 834.

[129] J. Kim, D. Son, M. Lee, C. Song, J.K. Song, J.H. Koo, D.J. Lee, H.J. Shim, J.H. Kim, M. Lee, T. Hyeon, D.H. Kim, A wearable multiplexed silicon nonvolatile memory array using nanocrystal charge confinement, Sci. Adv. 2 (2016) 1–10.

[130] J. Viventi, D.H. Kim, L. Vigeland, E.S. Frechette, J.A. Blanco, Y.S. Kim, A.E. Avrin, V.R. Tiruvadi, S.W. Hwang, A.C. Vanleer, D.F. Wulsin, K. Davis, C.E. Gelber, L. Palmer, J. Van Der Spiegel, J. Wu, J. Xiao, Y. Huang, D. Contreras, J.A. Rogers, B. Litt, Flexible, foldable, actively multiplexed, high-density electrode array for mapping brain activity in vivo, Nat. Neurosci. 14 (2011) 1599–1605.

[131] X. Dai, W. Zhou, T. Gao, J. Liu, C.M. Lieber, Three-dimensional mapping and regulation of action potential propagation in nanoelectronics-innervated tissues, Nat. Nanotechnol. 11 (2016) 776–782.

[132] Y. Kim, A. Chortos, W. Xu, Y. Liu, J.Y. Oh, D. Son, J. Kang, A.M. Foudeh, C. Zhu, Y. Lee, S. Niu, J. Liu, R. Pfattner, Z. Bao, T.-W. Lee, A bioinspired flexible organic artificial afferent nerve, Science 360 (2018) 998–1003 80-.

[133] H. Lee, S. Lee, W. Lee, T. Yokota, K. Fukuda, T. Someya, Ultrathin organic electrochemical transistor with nonvolatile and thin gel electrolyte for long-term electrophysiological monitoring, Adv. Funct. Mater. 29 (2019) 1906982.

[134] C. Yao, Q. Li, J. Guo, F. Yan, I.-M. Hsing, Rigid and flexible organic electrochemical transistor arrays for monitoring action potentials from electrogenic cells, Adv. Healthc. Mater. 4 (2015) 528–533.

[135] Y. Liang, F. Brings, V. Maybeck, S. Ingebrandt, B. Wolfrum, A. Pich, A. Offenhäusser, D. Mayer, Tuning channel architecture of interdigitated organic electrochemical transistors for recording the action potentials of electrogenic cells, Adv. Funct. Mater. 29 (2019) 1902085.

[136] Y. Liang, M. Ernst, F. Brings, D. Kireev, V. Maybeck, A. Offenhäusser, D. Mayer, High performance flexible organic electrochemical transistors for monitoring cardiac action potential, Adv. Healthc. Mater. 7 (2018) 1800304.

[137] A. Cerea, V. Caprettini, G. Bruno, L. Lovato, G. Melle, F. Tantussi, R. Capozza, F. Moia, M. Dipalo, F. De Angelis, Selective intracellular delivery and intracellular recordings combined in MEA biosensors, Lab Chip 18 (2018) 3492–3500.

[138] P.B. Kruskal, Z. Jiang, T. Gao, C.M. Lieber, Beyond the patch clamp: nanotechnologies for intracellular recording, Neuron 86 (2015) 21–24.

[139] H. Fu, K. Nan, W. Bai, W. Huang, K. Bai, L. Lu, C. Zhou, Y. Liu, F. Liu, J. Wang, M. Han, Z. Yan, H. Luan, Y. Zhang, Y. Zhang, J. Zhao, X. Cheng, M. Li, J.W. Lee, Y. Liu, D. Fang, X. Li, Y. Huang, Y. Zhang, J.A. Rogers, Morphable 3D mesostructures and microelectronic devices by multistable buckling mechanics, Nat. Mater. 17 (2018) 268–276.

[140] M.K. Choi, O.K. Park, C. Choi, S. Qiao, R. Ghaffari, J. Kim, D.J. Lee, M. Kim, W. Hyun, S.J. Kim, H.J. Hwang, S.H. Kwon, T. Hyeon, N. Lu, D.H. Kim, Cephalopod-Inspired miniaturized suction cups for smart medical skin, Adv. Healthc. Mater. 5 (2016) 80–87.

[141] C. Xie, Z. Lin, L. Hanson, Y. Cui, B. Cui, Intracellular recording of action potentials by nanopillar electroporation, Nat. Nanotechnol. 7 (2012) 185–190.

[142] B.X.E. Desbiolles, E. de Coulon, A. Bertsch, S. Rohr, P. Renaud, Intracellular recording of cardiomyocyte action potentials with nanopatterned volcano-shaped microelectrode arrays, Nano Lett. 19 (2019) 6173–6181.

[143] T. Cohen-Karni, B.P. Timko, L.E. Weiss, C.M. Lieber, Flexible electrical recording from cells using nanowire transistor arrays, Proc. Natl. Acad. Sci. Unit. States Am. 106 (2009) 7309–7313.

[144] J.Y. Oh, D. Son, T. Katsumata, Y. Lee, Y. Kim, J. Lopez, H.-C. Wu, J. Kang, J. Park, X. Gu, J. Mun, N.G.-J. Wang, Y. Yin, W. Cai, Y. Yun, J.B.H. Tok, Z. Bao, Stretchable self-healable semiconducting polymer film for active-matrix strain-sensing array, Sci. Adv. 5 (2019) eaav3097.

[145] P. Gutruf, R.T. Yin, K.B. Lee, J. Ausra, J.A. Brennan, Y. Qiao, Z. Xie, R. Peralta, O. Talarico, A. Murillo, S.W. Chen, J.P. Leshock, C.R. Haney, E.A. Waters, C. Zhang, H. Luan, Y. Huang, G. Trachiotis, I.R. Efimov, J.A. Rogers, Wireless, battery-free, fully implantable multimodal and multisite pacemakers for applications in small animal models, Nat. Commun. 10 (2019) 5742.

[146] J. Abbott, T. Ye, K. Krenek, R.S. Gertner, S. Ban, Y. Kim, L. Qin, W. Wu, H. Park, D. Ham, A nanoelectrode array for obtaining intracellular recordings from thousands of connected neurons, Nat. Biomed. Eng. 4 (2020) 232–241.

[147] J. Abbott, T. Ye, L. Qin, M. Jorgolli, R.S. Gertner, D. Ham, H. Park, CMOS nanoelectrode array for all-electrical intracellular electrophysiological imaging, Nat. Nanotechnol. 12 (2017) 460–466.

[148] X. Duan, R. Gao, P. Xie, T. Cohen-Karni, Q. Qing, H.S. Choe, B. Tian, X. Jiang, C.M. Lieber, Intracellular recordings of action potentials by an extracellular nanoscale field-effect transistor, Nat. Nanotechnol. 7 (2012) 174–179.

[149] J.F. Eschermann, R. Stockmann, M. Hueske, X.T. Vu, S. Ingebrandt, A. Offenhäusser, Action potentials of HL-1 cells recorded with silicon nanowire transistors, Appl. Phys. Lett. 95 (2009) 083703.

[150] Q. Qing, Z. Jiang, L. Xu, R. Gao, L. Mai, C.M. Lieber, Free-standing kinked nanowire transistor probes for targeted intracellular recording in three dimensions, Nat. Nanotechnol. 9 (2014) 142–147.

[151] B. Tian, T. Cohen-Karni, Q. Qing, X. Duan, P. Xie, C.M. Lieber, Three-dimensional, flexible nanoscale field-effect transistors as localized bioprobes, Science 329 (2010) 830–834 80-.
[152] Y. Zhao, S.S. You, A. Zhang, J.-H. Lee, J. Huang, C.M. Lieber, Scalable ultrasmall three-dimensional nanowire transistor probes for intracellular recording, Nat. Nanotechnol. 14 (2019) 783–790.
[153] H. Zhu, K.S. Scharnhorst, A.Z. Stieg, J.K. Gimzewski, I. Minami, N. Nakatsuji, H. Nakano, A. Nakano, Two dimensional electrophysiological characterization of human pluripotent stem cell-derived cardiomyocyte system, Sci. Rep. 7 (2017) 1–9.
[154] A. Mencattini, F. Mattei, G. Schiavoni, A. Gerardino, L. Businaro, C. Di Natale, E. Martinelli, From petri dishes to organ on chip platform: the increasing importance of machine learning and image analysis, Front. Pharmacol. 10 (2019) 1–4.
[155] K.L. Fetah, B.J. DiPardo, E.M. Kongadzem, J.S. Tomlinson, A. Elzagheid, M. Elmusrati, A. Khademhosseini, N. Ashammakhi, Cancer modeling-on-a-chip with future artificial intelligence integration, Small 15 (2019) 1–14.
[156] L. Grob, H. Yamamoto, S. Zips, P. Rinklin, A. Hirano-Iwata, B. Wolfrum, Printed 3D electrode arrays with micrometer-scale lateral resolution for extracellular recording of action potentials, Adv. Mater. Technol. (2019) 1–10 1900517.
[157] Y. Kubota, H. Oi, H. Sawahata, A. Goryu, Y. Ando, R. Numano, M. Ishida, T. Kawano, Nanoscale-tipped high-aspect-ratio vertical microneedle electrodes for intracellular recordings, Small 12 (2016) 2846–2853.